The Plant Cell, Vol. 14, 237–261, January 2002, www.plantcell.org © 2002 American Society of Plant Biologists

Reevaluation of the Effects of Brefeldin A on Plant Cells Using Tobacco Bright Yellow 2 Cells Expressing Golgi-Targeted Green Fluorescent Protein and COPI Antisera[W]

Christophe Ritzenthaler,[a,1,5] Andreas Nebenführ,[b,1,2] Ali Movafeghi,[c,1,3] Christiane Stussi-Garaud,[a] Leila Behnia,[c] Peter Pimpl,[c] L. Andrew Staehelin,[b] and David G. Robinson[c,4]

[a] Institut de Biologie Moléculaire des Plantes, 67084 Strasbourg Cedex, France
[b] Department of Molecular, Cellular, and Developmental Biology, University of Colorado, Boulder, Colorado 80309-0347
[c] Albrecht-von-Haller Institute of Plant Sciences, University of Göttingen, D-37073 Göttingen, Germany

Brefeldin A (BFA) causes a block in the secretory system of eukaryotic cells by inhibiting vesicle formation at the Golgi apparatus. Although this toxin has been used in many studies, its effects on plant cells are still shrouded in controversy. We have reinvestigated the early responses of plant cells to BFA with novel tools, namely, tobacco Bright Yellow 2 (BY-2) suspension-cultured cells expressing an in vivo green fluorescent protein–Golgi marker, electron microscopy of high-pressure frozen/freeze-substituted cells, and antisera against Atγ-COP, a component of COPI coats, and AtArf1, the GTPase necessary for COPI coat assembly. The first effect of 10 μg/mL BFA on BY-2 cells was to induce in $<$5 min the complete loss of vesicle-forming Atγ-COP from Golgi cisternae. During the subsequent 15 to 20 min, this block in Golgi-based vesicle formation led to a series of sequential changes in Golgi architecture, the loss of distinct Golgi stacks, and the formation of an endoplasmic reticulum (ER)–Golgi hybrid compartment with stacked domains. These secondary effects appear to depend in part on stabilizing intercisternal filaments and include the continued maturation of *cis*- and medial cisternae into *trans*-Golgi cisternae, as predicted by the cisternal progression model, the shedding of *trans*-Golgi network cisternae, the fusion of individual Golgi cisternae with the ER, and the formation of large ER-Golgi hybrid stacks. Prolonged exposure of the BY-2 cells to BFA led to the transformation of the ER-Golgi hybrid compartment into a sponge-like structure that does not resemble normal ER. Thus, although the initial effects of BFA on plant cells are the same as those described for mammalian cells, the secondary and tertiary effects have drastically different morphological manifestations. These results indicate that, despite a number of similarities in the trafficking machinery with other eukaryotes, there are fundamental differences in the functional architecture and properties of the plant Golgi apparatus that are the cause for the unique responses of the plant secretory pathway to BFA.

INTRODUCTION

The fungal toxin brefeldin A (BFA) has been used as an experimental tool to block secretion in a wide variety of eukaryotic cells (Fujiwara et al., 1988; Satiat-Jeunemaitre et al., 1996). In plants, it has been shown to block the secretion of cell wall polysaccharides and proteins (Driouich et al., 1993; Schindler et al., 1994; Kunze et al., 1995) as well as the transport of soluble proteins to the vacuole (Holwerda et al., 1992; Gomez and Chrispeels, 1993). In animals, the BFA-induced block of secretion is accompanied by a structural disruption of the secretory system, most notably involving the Golgi apparatus, which becomes extensively tubulated and eventually fuses with the endoplasmic reticulum (ER) (Sciaky et al., 1997; Hess et al., 2000). In contrast, the responses of plant cells to BFA range from a loss of *cis*-cisternae and a concomitant increase in *trans*-cisternae to the accumulation of Golgi membranes in highly vesiculated clusters, the so-called BFA compartments, and in some cases the fusion of the Golgi with the ER (Rutten and Knuiman, 1993; Satiat-Jeunemaitre et al., 1996; Driouich and Staehelin, 1997). The cause of this variability is unclear, but it has been speculated that it might reflect the existence of multiple binding sites for BFA in plants, so that, depending on the concentration of BFA, secretory traffic may be blocked either between the ER and the Golgi or between the

[1] These authors contributed equally to this article.
[2] Current address: Department of Botany, University of Tennessee, Knoxville, TN 37996-1100.
[3] Current address: Department of Plant Biology, Faculty of Natural Sciences, Tabriz University, Tabriz, Iran.
[4] Current address: Zellenlehre, Universität Heidelberg, D-69120 Heidelberg, Germany.
[5] To whom correspondence should be addressed. E-mail christophe.ritzenthaler@ibmp-ulp.u.strasbg.fr; fax 33-388-614-442.
[W] Online version contains Web-only data.
Article, publication date, and citation information can be found at www.plantcell.org/cgi/doi/10.1105/tpc.010237.

Golgi and the *trans*-Golgi network (Staehelin and Driouich, 1997).

In recent years, our understanding of the transport mechanisms underlying the secretory system and the action of BFA has increased greatly as a result of advances made with mammalian and yeast cells (Lippincott-Schwartz et al., 2000; Scales et al., 2000). For example, we now know that the transport of membranes and proteins between the ER and the Golgi apparatus, as well as transport within the Golgi apparatus, is mediated by COP-coated vesicles. Anterograde transport from the ER to the Golgi depends on COPII-coated vesicles, whereas retrograde transport from the Golgi to the ER and intra-Golgi transport is mediated by COPI-coated vesicles. The formation of these vesicles is basically a two-step process involving the sequential recruitment of a GTPase and a preformed coat protein complex, both of which are located mainly in the cytosol (Harter, 1999; Nickel and Brügger, 1999). Coat formation is triggered by the conversion of the GTPase in its GDP form to a GTP form, a process catalyzed by a membrane-associated GTP exchange factor (GEF) (Helms and Rothman, 1992). In the case of COPI-coated vesicles, the GTPase is ADP-ribosylation factor 1 (Arf1p) (Kahn and Gilman, 1986; Serafini et al., 1991), and the coat protein is a heptameric complex known as coatomer (Waters et al., 1991; Duden et al., 1994). Gea1/2p are the most probable GEFs for Arf1 (see reviews by Moss and Vaughn, 1998; Chavrier and Goud, 1999). BFA has been shown to inhibit the activation of Arf1 by locking this GTPase and its GEF in a nonproductive complex (Chardin and McCormick, 1999). One of the first effects of BFA on mammalian cells, therefore, is the rapid release of membrane-bound coatomer (Donaldson et al., 1990; Scheel et al., 1997), which is followed later by the absorption of Golgi membranes into the ER (Sciaky et al., 1997), although proteins of the Golgi matrix appear to stay behind (Seemann et al., 2000).

In this study, we tested whether this paradigm of BFA action also applies to plant cells. For this, we have taken advantage of two recent technical advances that have made it possible to analyze more accurately how BFA interacts with elements of the plant secretory pathway. The first is the development of plant cells expressing ER- and Golgi-targeted green fluorescent protein (GFP) constructs (Boevink et al., 1998; Nebenführ et al., 1999; Batoko et al., 2000), which enable changes in the morphology of the ER and Golgi to be monitored very precisely in living cells. The second is the production of antisera raised against recombinant plant COPI polypeptides, which have made it possible to establish that plant cells also possess coatomer (Movafeghi et al., 1999; Pimpl et al., 2000). These coatomer and a plant Arf1p homolog localize to the cytosolic surface of microvesicles seen budding from the periphery of Golgi cisternae (Pimpl et al., 2000).

In this investigation, we used tobacco Bright Yellow 2 (BY-2) cells expressing α-mannosidase 1–GFP (GmMan1-GFP, a marker for the Golgi apparatus) (Nebenführ et al., 1999) or GFP-HDEL (for visualization of the ER) (Nebenführ et al., 2000) to follow BFA-induced changes in Golgi and ER organization over time. The effects of BFA also were monitored biochemically and at the whole-cell level by both electron microscopy of high-pressure frozen/freeze-substituted cells and by confocal laser scanning microscopy using antisera against Atγ-COP and AtArf1p. Our data show that BY-2 cells react rapidly (<5 min) to low concentrations of BFA and that the initial effect of the toxin, as in animal cells, is the loss of coatomer from the Golgi cisternae. The resulting interruption of Golgi-based vesiculation leads to a series of secondary effects, such as the loss of cisternae and the fusion of the remaining cisternae with the ER. Long-term treatments (hours) lead to further structural changes in the ER-Golgi hybrid compartment. We also show that full recovery from a short BFA treatment (30 min) takes up to 2 hr.

RESULTS

BFA Leads to a Loss of Distinct Golgi Stacks in BY-2 Cells

In the absence of BFA, both living and fixed GmMan1-GFP cells displayed a punctate pattern of GFP fluorescence typical of the organization of Golgi stacks in plant cells (Figure 1A; see also Nebenführ et al., 1999, 2000). The stacks were distributed more or less evenly throughout the cytoplasm in the cell cortex, the transvacuolar strands, and the perinuclear region. Individual fluorescent spots appeared as either discs or bars depending on whether they were viewed face-on or edge-on, respectively (Nebenführ et al., 1999). Doughnut/ring-like fluorescent structures were observed rarely in untreated cells. We followed the changes in Golgi stack morphology and distribution in living cells maintained in a perfusion chamber during treatment with 10 μg/mL BFA (37.7 mM) by time lapse photography (Figure 1 and time lapse video sequence). In addition, we documented the morphological changes in fixed cells (Figure 2), because the rapid Golgi movements in living cells necessitated rapid image capture, which resulted in a loss of image quality. The fixation process did not affect the distribution of the GFP signal or the shape of the Golgi stacks (cf. video sequence and Figure 2).

The first visible change in Golgi morphology, as monitored by GmMan1-GFP, was the conversion of the disc-shaped Golgi images into ring-like images (video sequence at 11:59 min:sec; Figure 2B, inset). The doughnuts began to appear 5 min after the addition of BFA and remained visible for a period of 10 to 15 min. During and after this time, there was a progressive reduction in the numbers of free Golgi stacks concomitant with the formation of highly fluorescent aggregates (video sequence from 9:41 to 14:52; Figures 2C to 2E) and a fainter fluorescent network (Figure 2D). This network

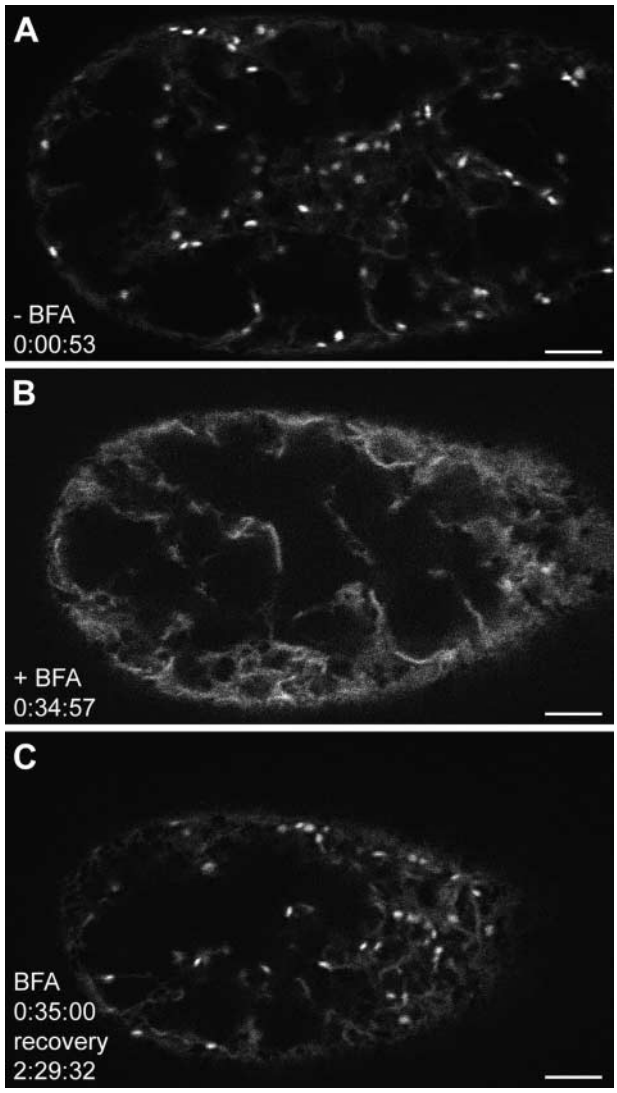

Figure 1. Time Lapse Confocal Observation of a Single BY-2 Cell Expressing GmMan1-GFP during BFA Treatment and Subsequent Recovery.

The cell was captured in the cortical cytoplasm close to the plasma membrane. It appears smaller at later time points because it settled slightly during the observation period. Cells were maintained in a perfusion chamber, and GFP fluorescence was captured with a confocal microscope at 34-, 64-, and 124-sec intervals as indicated (hours:minutes:seconds). See supplemental data for video at www.plantcell.org.

(A) Golgi stacks are clearly visible as bright fluorescent spots before BFA treatment. Some fluorescence also is found in a fine network, indicating the presence of a subset of the marker molecules in the ER.

(B) After 35 min in medium containing 10 μg/mL BFA, no Golgi stacks are visible. The increased ER fluorescence is caused by the relocation of the GmMan1-GFP marker into that organelle. After this time, the supply of medium is switched to fresh Murashige and Skoog medium (1962) without the toxin.

(C) During the recovery, fluorescent Golgi stacks first begin to appear after ~60 min, although their numbers remain low until 2 hr after the removal of BFA.

Bars = 5 μm.

extended throughout the cell and closely resembled the ER in untreated BY-2 cells expressing GFP-HDEL (data not shown). The gradual loss of Golgi stacks and the simultaneous increase in ER-like fluorescence are indicative of a redistribution of the GmMan1-GFP Golgi marker into the ER. Although some of the ER-like fluorescence may have resulted from newly synthesized GFP in the ER, the speed with which the fluorescent network appeared suggests that this new pool of GmMan1-GFP does not contribute significantly to the signal. These observations are consistent with those made by Boevink et al. (1998) in BFA-treated tobacco leaf epidermis cells. By 30 min, individual Golgi stacks were seen rarely, especially in the cortical cytoplasm, with the fluorescence being either in the ER-like network or concentrated in perinuclear pleiomorphic aggregates up to 5 μm in size (Figure 2E). In all of our experiments, we observed a remarkable variability in the rate of response of the cells to BFA within a culture. Although all cells followed the sequential changes described above, the BFA-induced changes occurred at different rates for different cells. Even the Golgi stacks within a given cell showed some variability, albeit to a lesser extent than in those between cells (data not shown).

Golgi Stacks in BFA-Treated Cells Lose Cisternae in a *cis*-to-*trans* Direction

To further characterize the morphological changes in Golgi architecture in response to BFA, we examined ultrathin sections of high-pressure frozen/freeze-substituted cells at various times during the treatment. Golgi stacks in untreated BY-2 cells expressing the Golgi marker GmMan1-GFP had on average 5.2 ± 0.1 cisternae (mean ±SE, $n = 50$). In most stacks, the *cis*-, medial, and *trans*-cisternae were distinguished based on their staining patterns (Figure 3A), as described previously (Zhang and Staehelin, 1992). Intercisternal elements were visible only between *trans*-cisternae or between medial and *trans*-cisternae (Figure 3A, arrowhead), a distribution that also has been described for Golgi stacks in sycamore maple cells (Driouich et al., 1993) and Arabidopsis and tobacco root tip cells (Staehelin et al., 1990). Distinct COP-type protein coats were seen on budding vesicle profiles in the periphery of the cisternae (data not shown), but their numbers were low.

Cells treated with 10 μg/mL BFA for 5 min before high-pressure freezing showed an average loss of 1.8 cisternae

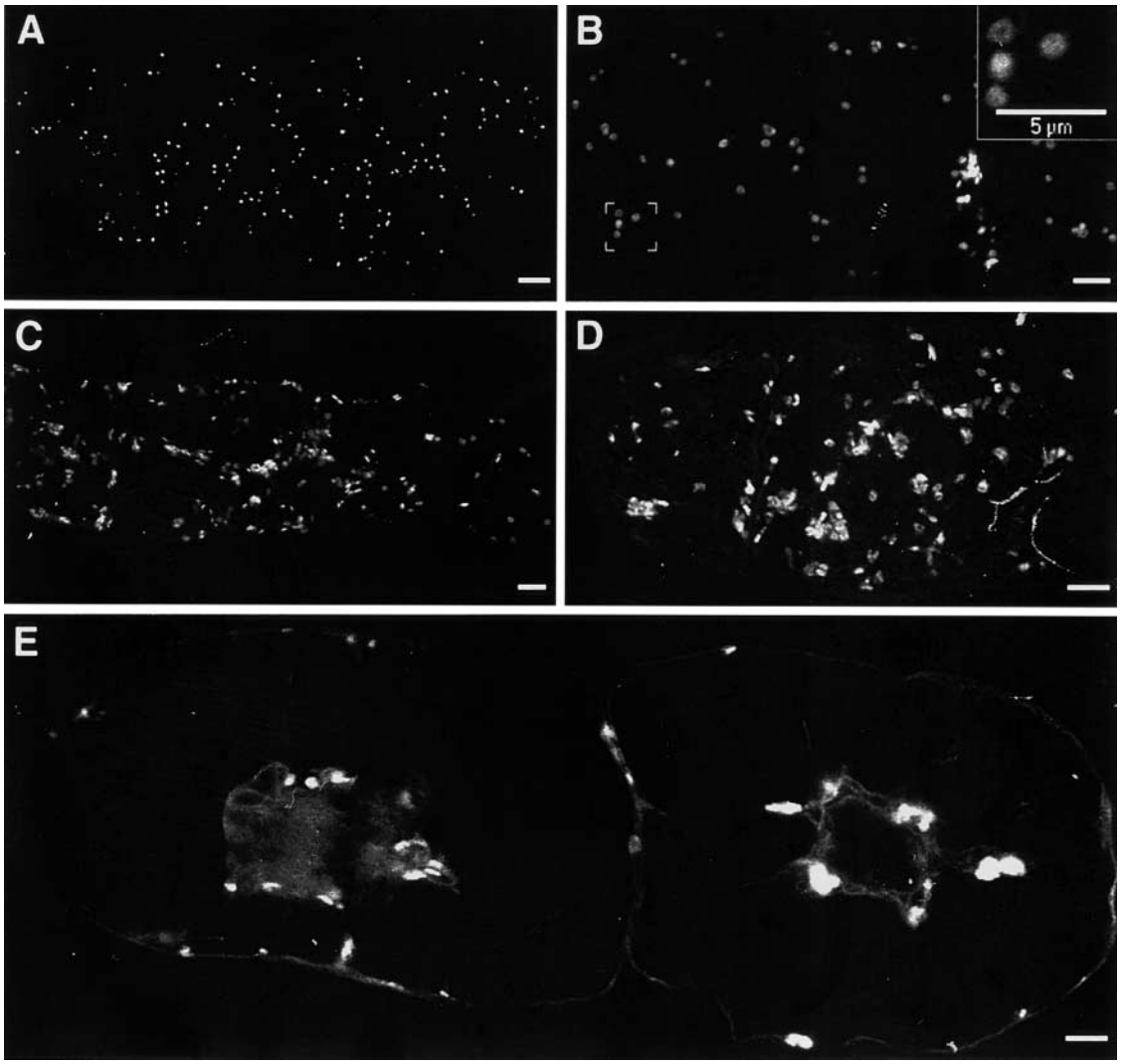

Figure 2. BFA-Induced Changes in GmMan1-GFP Fluorescence in Fixed Cells.

(A) In the absence of BFA, GmMan1-GFP cells display a punctate pattern of GFP fluorescence typical of the organization of Golgi stacks in plant cells.
(B) Conversion of the disc-shaped Golgi images into ring/doughnut-like images at 5 min after the addition of BFA at 10 μg/mL. The inset shows a higher magnification of the boxed region clearly showing the ring-like structure of some Golgi stacks.
(C) and **(D)** GFP fluorescence at 10 and 15 min after BFA treatment. Most Golgi stacks appear aggregated.
(E) Perinuclear pleiomorphic aggregates observed in GmMan1-GFP cells at 30 min after BFA addition.
All images are single optical confocal microscopy sections of fixed tobacco BY2 cells. **(A)** to **(D)** show sections through the cortical cytoplasm. **(E)** shows a section through the middle of two cells. Bars = 5 μm.

per Golgi stack (Figure 4). On the basis of the staining pattern of the remaining cisternae, this reduction was caused by the loss of *cis*-cisternae (Figure 3B). Thus, only 25% of Golgi stacks had discernible *cis*-cisternae after 5 min in BFA, compared with 86% in untreated cells. The percentage of stacks with *cis*-cisternae decreased even further to 9% after 10 min in BFA.

In BFA-Treated Cells, ER Membranes Adhere to Golgi Stack Remnants to Form Hybrid Stacks

Starting as early as 5 min into the BFA treatment, we observed ER cisternae adhering to Golgi stacks, forming ER-Golgi hybrid stacking domains (Figures 3C, 3D, 3F, and 4). Identification of the Golgi-associated ER membranes was

based on the presence of ribosomes on contiguous membrane regions (Figures 3C and 3F). Stacked ER cisternae were first seen on one side of the residual Golgi stacks (Figures 3C and 3D), but later they were found on both sides (Figures 3F and 4). Such ER-Golgi "sandwiches" began to appear after 10 min in BFA and became the predominant form of hybrid stacks after 20 min of treatment (Figure 4). Interestingly, the average number of cisternae per stack did not change during this period, irrespective of their appearance as Golgi or ER like (Figure 4).

The Golgi stacks with at least two cisternae remaining after 10 to 30 min of treatment with BFA usually had clearly discernible electron-dense regions between their Golgi-like cisternae (Figure 3E, arrowheads). The presence of these intercisternal elements is consistent with the interpretation that the remaining cisternae are mostly of the *trans*-Golgi type and suggests that these elements mechanically stabilize the cisternae. Interestingly, short intercisternal elements also were found between typical Golgi cisternae and ER-like cisternae in ER-Golgi hybrid stacks (Figure 3F, arrowheads). Thus, during the initial BFA response phase, the Golgi stacks lost cisternae in a *cis*-to-*trans* direction, whereas during the second phase, the top and bottom cisternae of the residual Golgi stacks seemed to be "replaced" with cisternae that exhibited characteristics of both ER (membrane staining, ribosomes) and Golgi (stacking, intercisternal elements) membranes.

The sequence of events described here represents the aggregate of observations of many stacks in many cells. Individual cells appear to progress through this sequence at different rates, as shown by the variability of structures seen in each sample. At the same time, Golgi stacks within a given cell showed much less variability in their response. This is consistent with the live cell observations described in the previous section.

ER Morphology Changes as Golgi Stacks Disappear

After 20 min of exposure of the cells to BFA, the number of Golgi stack remnants decreased rapidly and it became difficult to find them in thin sections. Instead, in a number of cells, groups of sheet-like ER cisternae became organized into wide stacks with flared margins (Figure 5A). These regions of "stacked ER" cisternae were located almost exclusively in the perinuclear region of the cells. The nonstacked regions of these ER cisternae often were unusually straight and had more ribosome-free membranes than control cells (75% of contour length after 30 min of BFA treatment, 66% in untreated cells). In addition, these ER cisternae frequently appeared dilated and contained electron-dense material (Figure 5A, open arrow). The dilated domains usually were bounded by membranes with wide, smooth curves that were never observed in untreated cells (Figure 5B, arrows). Potentially active ER export sites could be recognized in the form of coated budding vesicles on ribosome-free ER membrane domains in cells treated for 30 min or 5 hr with BFA (Figures 5C and 5D, arrowheads).

Some cells also contained aggregates of Golgi stack remnants and large numbers of associated vesicles that showed a staining pattern similar to that seen in Golgi-derived secretory vesicles in untreated cells (Figure 5B). Thus, these aggregates, which always were found near the nucleus, had the same appearance as BFA compartments described in other systems (Satiat-Jeunemaitre et al., 1996). Interestingly, cells that displayed such BFA compartments did not contain stacked ER-like cisternae, although they were able to form the smoothly curved ER domains. This finding suggests that tobacco BY-2 cells can respond to BFA in two ways that are, in part, mutually exclusive. Thus, in parallel with the BFA-induced loss of Golgi stacks, some cells start producing unusual ER-Golgi hybrid stacks, whereas others develop aggregates of Golgi remnants and secretory vesicles.

Formation of the Stacked ER-Golgi Hybrid Compartment Also Occurs in BFA-Treated Wild-Type Tobacco Cells

To determine whether the morphological changes described here were caused by the presence of the *cis*-Golgi marker GmMan1-GFP in the Golgi stacks, we also investigated the effects of BFA on wild-type BY-2 cells and on tobacco root cap cells, both of which contain Golgi with intercisternal elements. As documented in Figures 6A and 6B, BFA induced the same structures in both wild-type and transformed BY-2 cells. However, the wild-type BY-2 cells responded on average faster than did the transgenic cells. The most visible difference between the BY-2 cell lines was that ER-Golgi hybrid stacks appeared to be more stable in wild-type cells and developed into much larger aggregates (Figures 6A and 6B) (Yasuhara et al., 1995). These perinuclear hybrid stacks were seen to reach lengths of 8 μm and contained up to 10 stacked cisternae. At early time points during the BFA treatment (10 to 15 min), the hybrid stacks tended to be short and exhibited the same sandwiching of *trans*-Golgi cisternae between flanking ER cisternae seen for the transgenic Golgi (Figure 6A). After 60 min, the hybrid stacks became longer and thicker, apparently by lateral fusion and vertical adhesion between hybrid stacks (Figure 6B) and the addition of new cisternae. In these large hybrid stacks, the stiff island-like domains of the original Golgi membranes could be identified by both the presence of intercisternal elements and the stronger staining of the membranes (Figures 6A and 6B). Indeed, these residual Golgi cisternae seemed to form the focal points around which the larger hybrid stacks formed. Unlike in the transgenic line, we were unable to find any BFA compartments in BFA-treated wild-type BY-2 cells.

To further confirm the formation of ER-Golgi hybrid stacks in plant cells exposed to BFA, we treated root tips of tobacco seedlings with 50 μg/mL BFA (178.5 mM) for up to 2 hr. Hybrid stacks consisting of ER-like membranes adhering to residual stacks of *trans*-like Golgi cisternae were observed

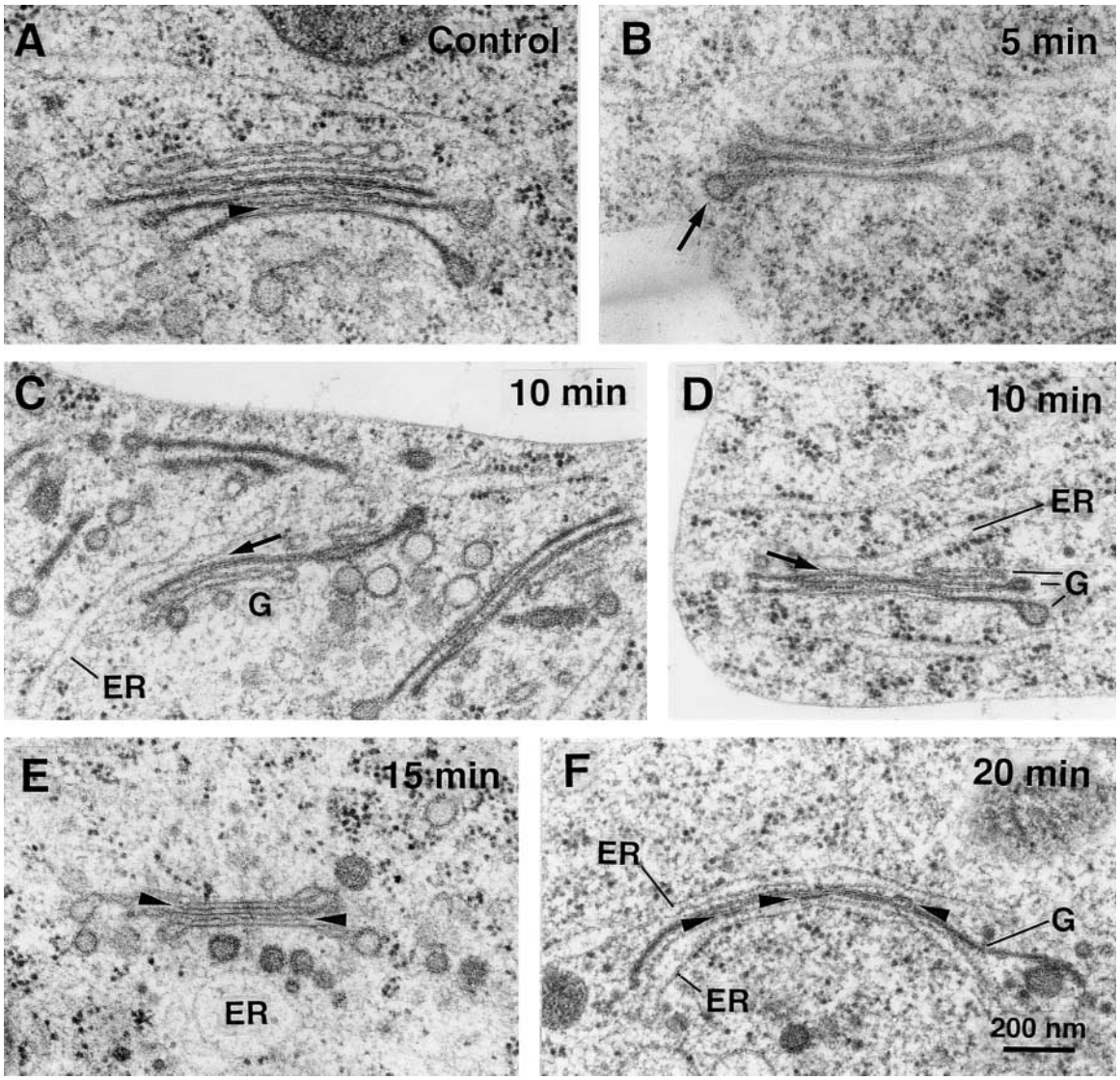

Figure 3. Short-Term Effects of BFA on the Morphology of Golgi Stacks in BY-2 Cells.

Electron micrographs of Golgi stacks in high-pressure frozen/freeze-substituted BY-2 cells before **(A)** or early during (**[B]** to **[F]**) BFA treatment.
(A) Control. Typical appearance of a Golgi stack in untreated BY-2 cells. The stack has a clear *cis*-to-*trans* polarity indicated by the differences in membrane staining and cisternal morphology. Intercisternal elements (arrowhead) are seen only between *trans*-cisternae.
(B) BFA (5 min). This Golgi stack consists of only three cisternae that all have medial or *trans* appearance (cf. with **[A]**). Part of a clathrin coat still is present at one of the cisternae (arrow). The ER morphology is not altered at this time.
(C) BFA (10 min). Golgi (G) remnants that consist of only medial- and *trans*-like cisternae often are surrounded by accumulations of vesicles that appear to have originated at the *trans*-Golgi network. One of the stacks in this image has an ER cisterna associated with it (arrow).
(D) BFA (10 min). A clear example of an ER cisterna stacked onto a Golgi cisterna of medial/*trans* appearance (arrow).
(E) BFA (15 min). At this time, most cisternae resemble *trans*-cisternae and carry intercisternal filaments between them (arrowheads). Note the large number of Golgi-derived vesicles in the vicinity of the stack. The dilated membrane-bound compartment near the bottom appears to be ER because it has ribosomes associated with it.
(F) BFA (20 min). A single *trans*-like cisterna sandwiched between two ER cisternae (note the ribosomes on the outer membrane). Short patches of intercisternal filaments are present between the cisternae (arrowheads).

in root cap cells (Figure 6C). As described above for the hybrid stacks in BY-2 cells, intercisternal filaments were prominent between these cisternae (Figure 6C, arrowheads). Thus, the stacking of ER cisternae onto Golgi stack remnants occurs in both nondifferentiated (suspension-cultured) and differentiated tobacco cells.

Long-Term Treatment with BFA Leads to Radical Alterations in the Morphology of the ER-Golgi Hybrid Compartment

Long-term treatment (>3 hr) of GmMan1-GFP–expressing cells with BFA resulted in the formation of a highly abnormal fluorescent membrane compartment (Figure 7A) that bore little resemblance to any of the ER or Golgi structures seen after shorter treatment times. This secondary type of ER-Golgi hybrid compartment consisted of thin tubules connecting to sharply delineated, rounded, and highly fluorescent domains that frequently exhibited a sponge-like pattern (Figure 7A). Ultrastructural analysis of cells treated with BFA for 5 hr revealed that these cells displayed two unusual ER morphologies with common features (Figures 7B and 7C). The more frequently observed conformation consisted of a semiregular lattice of ER membranes with smoothly curved round membrane profiles and a swollen lumen with fine filamentous contents (Figure 7B, arrows). Less frequently seen were the stacked cisternal structures with membrane-bound polysomes, as illustrated in Figure 7C. Typically, the membranes in these stacks appeared cemented together by a layer of darkly stained material that resembled disorganized intercellular element structures (Figure 7C, arrowheads). The nonstacked ER domains connecting to the stacks also exhibited distinctly rounded contours and extended into straight tubular or sheet-like profiles (Figure 7C). Thus, BY-2 cells that were treated with BFA for >3 hr contained an ER-Golgi hybrid compartment with grossly abnormal morphology.

Atγ-COP and AtArf1p Are Localized to the Periphery of Golgi Stacks

Studies of mammalian cells have established that BFA interacts with the guanine nucleotide exchange factor, thereby inhibiting Arf1p recruitment onto Golgi membranes and thus preventing coatomer assembly on budding vesicles (see Introduction). Similar findings have been reported in an in vitro study of COPI assembly on plant Golgi membranes (Pimpl et al., 2000), but the BFA concentrations required to block the in vitro COPI coat assembly in that investigation were 10-fold higher than that used in this in vivo study. To determine whether BFA at 10 μg/mL is able to affect membrane recruitment of coatomer and Arf1p in vivo, we first determined the intracellular distributions of γ-COP, a coatomer subunit, and Arf1p in transgenic GmMan1-GFP and GFP-HDEL BY-2

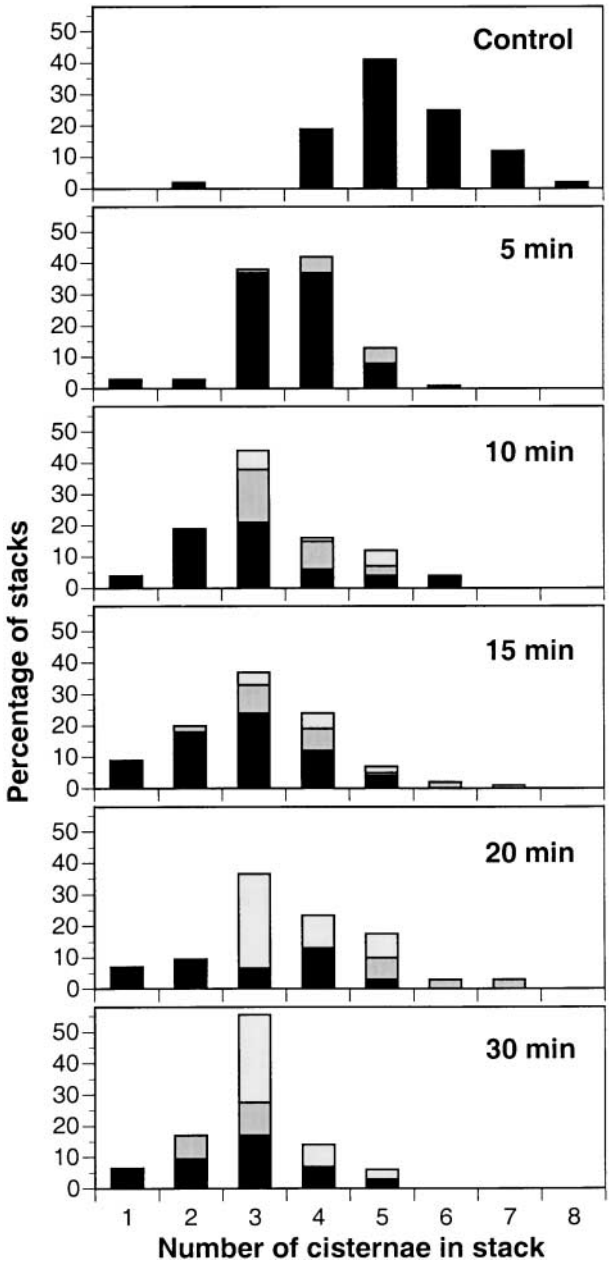

Figure 4. Histograms Depicting the Loss of Cisternae from Golgi Stacks during the First 30 min of BFA Treatment.

The percentage of stacks with a given number of cisternae was determined by examining electron micrographs of 29 to 112 stacks per time point. Stacks are characterized as containing only typical Golgi cisternae (black), containing one ER cisterna (dark gray), or containing two ER cisternae (light gray). Note the rapid shift in the distribution to thinner stacks within the first 5 to 10 min and the subsequent gradual increase of ER cisternae associated with the remaining stacks.

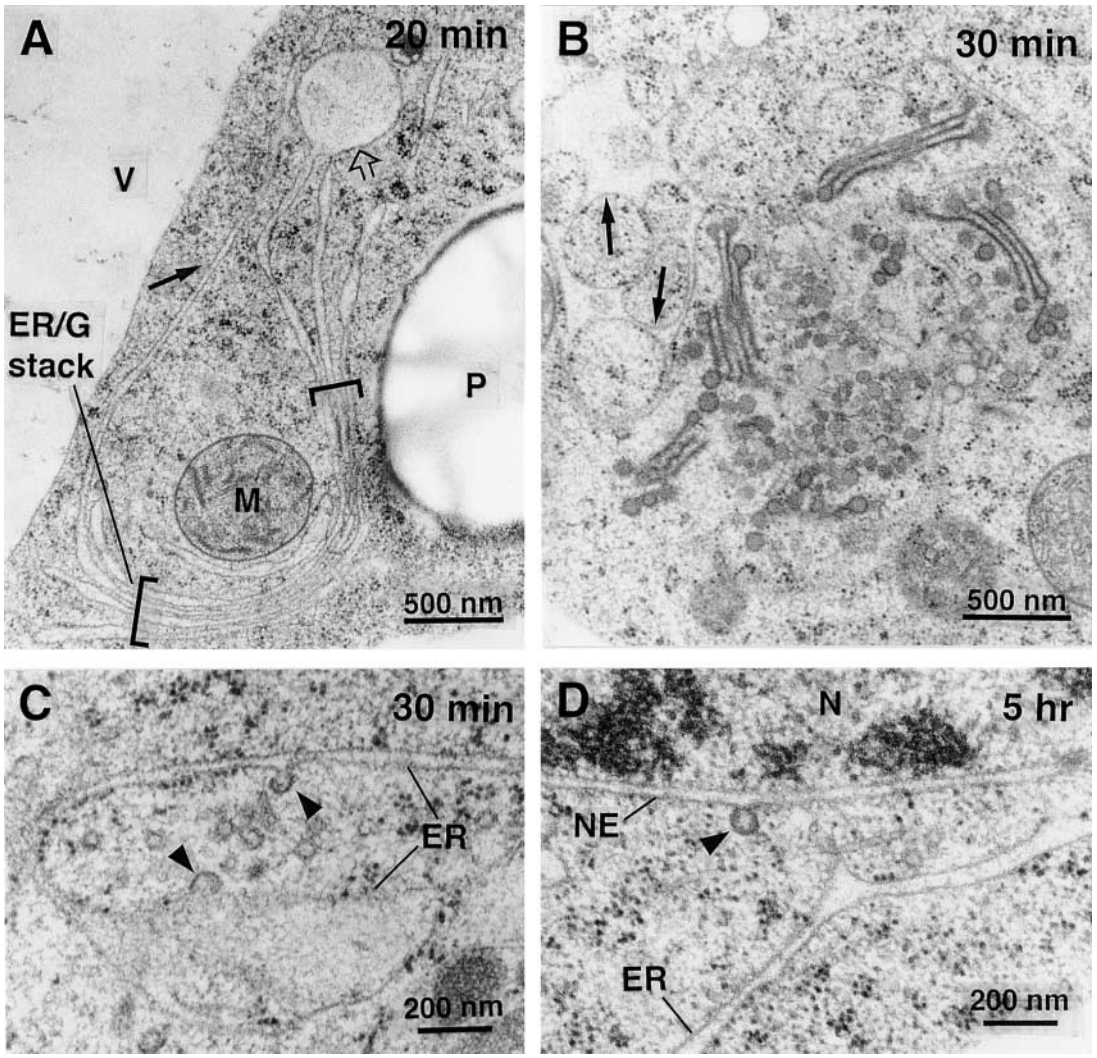

Figure 5. Effects of BFA on BY-2 Cells That Have Been Treated with BFA for Longer Periods.

(A) BFA (20 min). Some cells contain regions of stacked ER cisternae, usually in a perinuclear location. These cisternae are continuous with ER that has an abnormally straight appearance and more ribosome-free areas (arrow). Some domains of the ER are greatly inflated and contain electron-dense material (open arrow). G, Golgi; M, mitochondrion; P, plastid; V, vacuole.

(B) BFA (30 min). A subset of cells does not form the large stacked ER domains shown in **(A)** but contains clusters of Golgi stack remnants and large aggregations of Golgi-derived vesicles, similar to the BFA compartments described in other systems (see text). The ER in these cells also has an abnormal morphology, with electron-dense material in its dilated lumen and a large bending radius of its fenestrated membranes (arrows, upper left).

(C) BFA (30 min). ER export sites depicting budding coated vesicles (arrowheads) and several detached vesicles in the adjacent cytoplasm.

(D) BFA (5 hr). Coated budding vesicle (arrowhead) associated with the outer membrane of the nuclear envelope (NE), an ER equivalent membrane system. N, nucleus.

cells before and during BFA treatment using antibodies raised against Atγ-COP and AtArf1p proteins.

Immunofluorescence labeling with Atγ-COP and AtArf1p antisera was performed under conditions that did not alter the GFP fluorescence (Figure 2). Labeling was found to be highly specific, because no signal was detected in cells in which the primary antibody was omitted (data not shown). By comparing the immunofluorescence signals specific to both Atγ-COP and AtArf1p with that of GmMan1-GFP, it became clear that both of these proteins colocalized with the

Golgi stacks (Figures 8A to 8F). However, small differences in Atγ-COP versus AtArf1p labeling were observed: Atγ-COP labeling was consistently weaker and its distribution around individual Golgi stacks generally was more irregular than that of AtArf1p (cf. Figures 8B and 8C with 8E and 8F). In spite of being clearly Golgi associated, the Atγ-COP and AtArf1p labeling did not colocalize directly with the GmMan1-GFP fluorescence, as revealed by the very few yellow areas in the merged images (Figures 8C and 8F). Instead, Atγ-COP and AtArf1p labeling typically was ring shaped and confined to the periphery of the Golgi stacks (Figures 8A to 8F). This is most evident at higher magnification, at which the COPI-specific signal is seen as a red halo around the green GFP label of the Golgi stacks (Figure 8G). The distribution of coatomer around the perimeter of the Golgi stacks was mirrored by the AtArf1p signal (Figure 8H). This localization of AtArf1p is further illustrated by the fluorescence profile across one of the Golgi stacks (Figure 8I). The GmMan1-GFP signal followed a typical Gaussian curve (Figure 8I, green curve), whereas the AtArf1p signal along the same line reached maxima on either side of the GmMan1-GFP peak (Figure 8I, red curve).

To further ascertain the localization of Atγ-COP and AtArf1p around Golgi stacks and to evaluate their relationship to the ER, we also performed immunofluorescence labeling on transgenic GFP-HDEL cells with Atγ-COP (Figures 8J to 8L) and AtArf1p (data not shown) antisera. As in GmMan1-GFP cells, Atγ-COP fluorescence appeared punctate, forming small rings throughout the cortical region of the cell (Figure 8K). Compared with the GFP-HDEL distribution (Figure 8J), Atγ-COP–labeled structures rarely overlapped the ER but were found in close proximity to the thin tubules and sheets of the cortical ER. This type of spatial relationship between the ER and Golgi corresponds to that reported previously by Boevink et al. (1998) for tobacco epidermal cells. Together, the immunolabeling results with Atγ-COP and AtArf1p are in complete agreement with those obtained recently on cryosections of Arabidopsis and maize root cells using the same antisera (Pimpl et al., 2000). In both systems, the COPI coat–forming molecules were localized to the perimeter of the *cis* side of the Golgi stacks.

BFA Treatment Results in a Rapid Loss of Coatomer from Golgi Stacks

The effect of BFA on the localization of Atγ-COP and AtArf1p was investigated by both subcellular fractionation (Figure 9A) and immunofluorescence techniques (Figure 10). Within 5 min of the application of BFA, the membrane-bound form Atγ-COP was no longer detected in protein gel blots (Figure 9A). This result was the same for wild-type BY-2 cells and for the two transformants. In contrast, the intensity of the AtArf1p blot signal for the same total membrane fraction remained almost unchanged during the first 15 min of treatment, becoming markedly weaker only after 30 min of exposure to BFA. As judged by the lack of effect on the ER lumen marker BiP (binding protein), BFA appeared to perturb only proteins associated with the cytosolic membrane surface (Figure 9A). A corresponding increase in the amounts of immunodetectable Atγ-COP and AtArf1p in cytosolic fractions was barely detectable on protein gel blots from BFA-treated cells (Figure 9A). This lack of a clearly visible change most likely is attributable to the relatively high concentration of these proteins in the cytosol, which makes it difficult to register small increases in coatomer/Arf1p against a high background.

We confirmed and extended these biochemical data by confocal microscopy. Within 5 min after the application of 10 μg/mL BFA, Golgi-associated Atγ-COP labeling had disappeared almost completely in GmMan1-GFP cells, although at this time individual Golgi stacks in the cell cortex still were identified easily (Figures 10A to 10D). Instead, Atγ-COP labeling was dispersed throughout the cytoplasm or was present in small punctate structures rarely associated with the Golgi stacks (Figure 10A). This was particularly evident at high magnifications, at which typical BFA-induced GmMan1-GFP doughnuts were visible (Figure 10B) but with barely any associated Atγ-COP fluorescence (Figures 10C and 10D). In contrast, 5 min of BFA treatment resulted in only a reduction, and not a complete loss, of Golgi-associated AtArf1p labeling, together with the appearance of brightly fluorescent spots in the cytoplasm (Figure 10E). A detailed analysis of the AtArf1p fluorescence labeling revealed a faint halo (Figure 10G) around most BFA-induced GmMan1-GFP doughnuts (Figures 10F and 10H), but this halo was distinctly lighter than in the untreated cells (Figure 8E). After 20 min of BFA treatment, a diffuse fluorescence for AtArf1p was observed throughout the cytoplasm in the GmMan1-GFP cell line (Figure 10J). This fluorescence, however, was particularly intense around the perinuclear GmMan1-GFP pleiomorphic aggregates (Figures 10I and 10K). Parallel investigations of the GFP-HDEL cell line showed that, during a 20-min treatment period, BFA induced similar changes in the redistribution of Atγ-COP and AtArf1p fluorescence signals (Figures 10L to 10P). In both cases, only a diffuse cytoplasmic signal was observed, during which time the typical GFP-HDEL fluorescence of the ER remained unchanged.

BFA Effects on Golgi Stacks in BY-2 Cells Can Be Reversed Only Slowly

To investigate the reversibility of the short-term effects of BFA on BY-2 cell Golgi, GmMan1-GFP cells were treated for 20 to 30 min with BFA (10 μg/mL), washed, and then transferred to fresh growth medium. As described above, after 20 to 30 min of BFA treatment, individual Golgi stacks were no longer discernible (video sequence and Figures 1 and 2) and COPI coat proteins were no longer found in the membrane fraction (Figure 9A). Reformation of fluorescent Golgi stacks

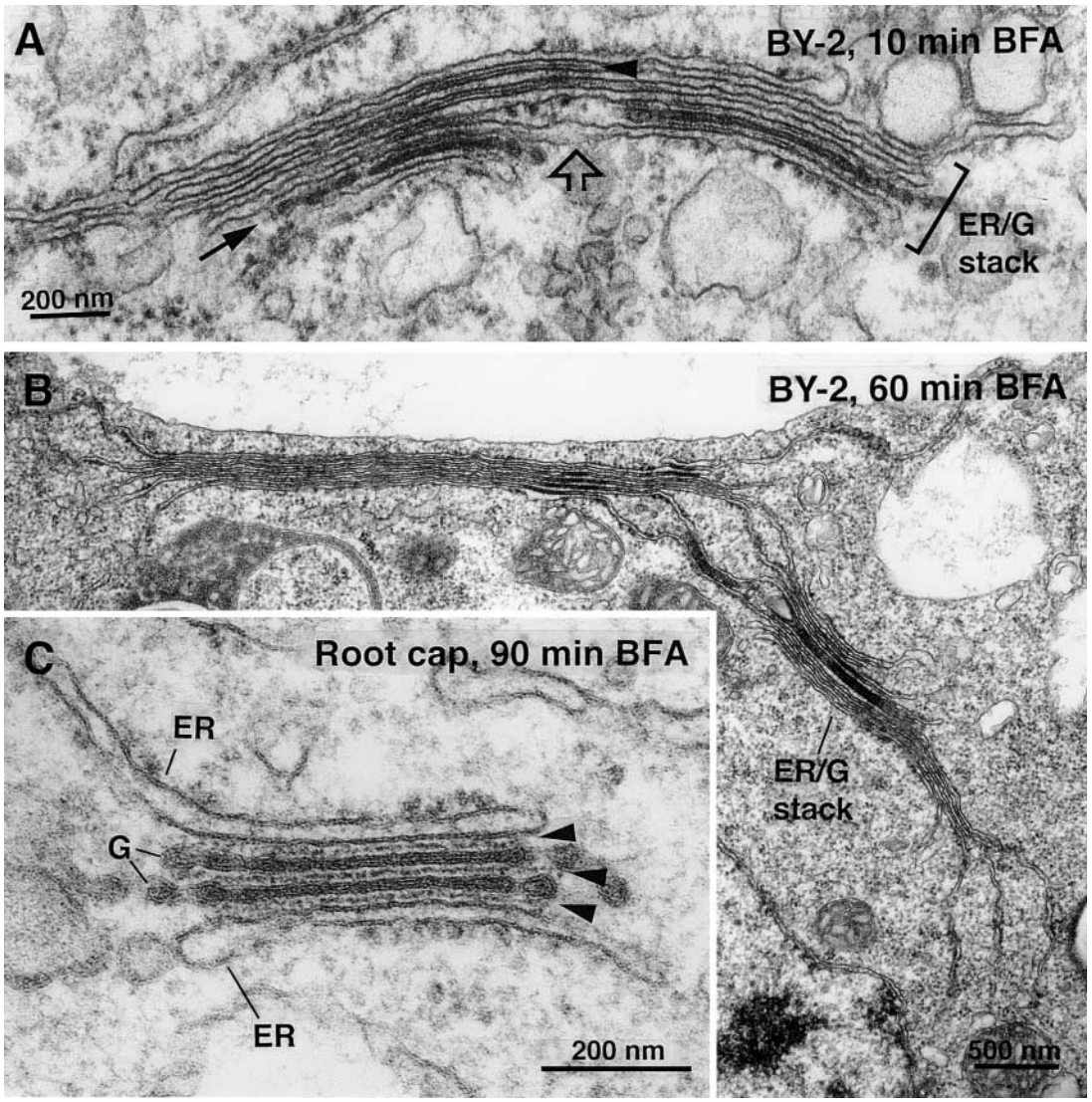

Figure 6. Effects of BFA Treatment on Nontransformed BY-2 Cells and Tobacco Root Cap Cells Preserved with Conventional Fixation.

(A) BFA (10 min). An ER-Golgi hybrid stack in a nontransformed BY-2 cell. Note the presence of intercisternal filaments between ER-like cisternae (arrowhead). This stack seems to have been formed by the lateral fusion of two stacks. The original stacks contain one *trans*-like cisterna each (arrow) and are connected by a loosely stacked region (open arrow).

(B) BFA (60 min). A large perinuclear ER-Golgi hybrid stack in a nontransformed BY-2 cell. Note the continuity of virtually all stacked cisternae with the ER. Tightly stacked regions alternate with single cisternae.

(C) BFA (90 min of 50 μg/mL BFA in tobacco root cap cell). An ER-Golgi hybrid stack with two *trans*-like cisternae sandwiched between two ER-like cisternae. Note the prominent intercisternal filaments between all cisternae (arrowheads).

was observed ~30 to 60 min after removal of the toxin (cf. video sequence). To determine whether these stacks were functionally competent with respect to vesicle formation, we processed them for subcellular fractionation (Figure 9B) and immunofluorescence (Figure 11) at various times during recovery. Protein gel blots (Figure 9B) clearly demonstrate the gradual recruitment of Atγ-COP onto membranes between 30 and 60 min after BFA removal. However, complete recovery took even longer, as shown by the fact that control levels of Atγ-COP were reached only after 90 min. A corre-

sponding recovery for AtArf1p on protein gel blots was not possible to record because the cells still retained significant levels of membrane-bound AtArf1p after 20 min of BFA treatment (see above and Figure 9A).

Confocal microscopy data corroborated and extended the biochemical measurements on recovery from BFA treatment. After 2 hr of incubation with fresh medium, mobile Golgi stacks again were observed in the majority of cells (Figures 11A and 11D and video sequence). In these cells, Atγ-COP (Figures 11B and 11C) and AtArf1p labeling (Figures 11E to 11F) were very similar to those obtained in untreated cells (Figure 8), indicating that the cells had recovered completely from BFA treatment within the 2-hr period. After only 1 hr, however, the degree of recovery of different cells in a given culture was variable, as illustrated in Figures 11G and 11H, which depict two neighboring cells from the same experiment. Whereas in the upper cell a nearly normal coincidence of AtArf1p and GmMan1-GFP labeling is seen, the lower cell shows GmMan1-GFP–labeled Golgi stacks but AtArf1p fluorescence still dispersed throughout the cortical cytoplasm. This diffuse cytosolic AtArf1p fluorescence was confirmed at higher magnification (Figures 11I to 11K), indicating that recovery is variable among cells in the range of 1 to 2 hr. Interestingly, sister cells, which resulted from a recent cell division and which still shared a common cell wall, usually recovered at similar rates and displayed similar AtArf1p labeling (Figure 11H). BY-2 cells recovering from BFA also were processed for electron microscopy. Golgi stacks typical of control cells were observed after 2 hr (data not shown). These data indicate that the plant Golgi apparatus can recover fully from BFA treatment within 2 hr but that the Golgi stack morphology is attained earlier than the ability to form significant numbers of COPI-coated vesicles.

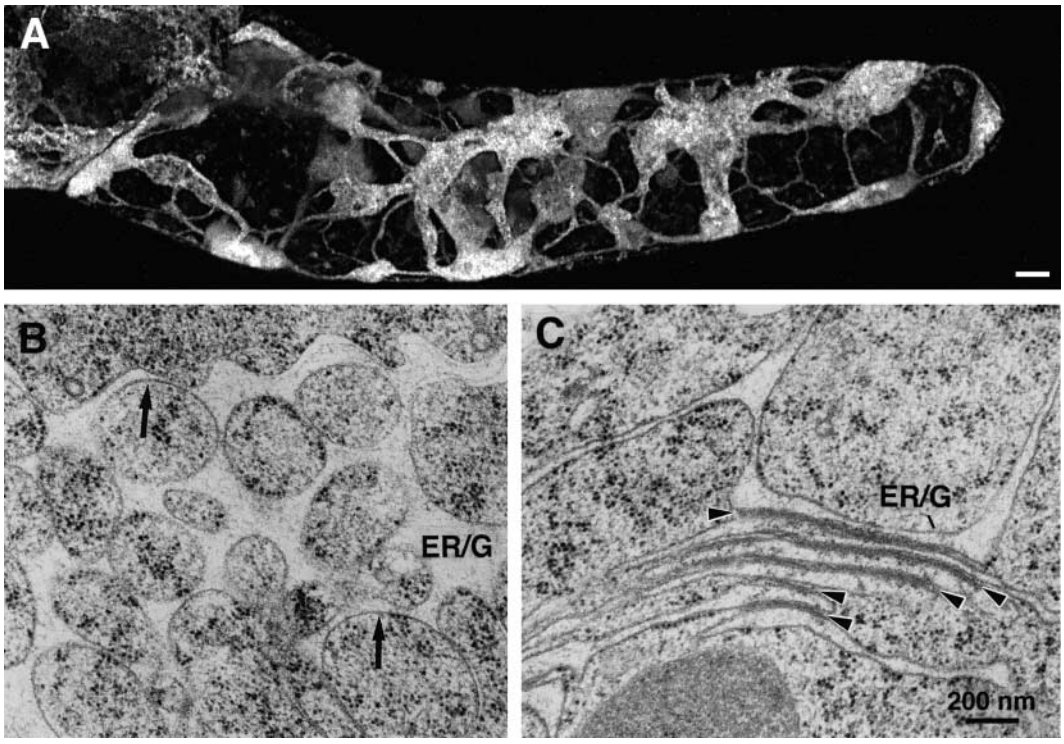

Figure 7. Long-Term Effects of BFA Treatment (5 hr) on the Morphology of the ER-Golgi Hybrid Compartment.

(A) Confocal reconstruction of the distribution of GmMan1-GFP fluorescence in an entire BY-2 cell treated with BY-2 for 5 hr (the projection was made from 113 consecutive 0.45-μm-thick optical sections). The ER-Golgi hybrid membrane system consists of large sheet-like domains with sponge-like substructure that are connected by thin tubules. Bar = 5 μm.

(B) Electron micrograph of an ER-Golgi hybrid compartment after 5 hr in BFA (high-pressure frozen sample). The membranes resemble a fenestrated sheet with unusually large openings and exhibit very smooth and evenly curved contours (arrows). The inflated lumen contains electron-dense material.

(C) In some instances, the ER-Golgi hybrid compartment after 5 hr in BFA (high-pressure frozen samples) contained regions of stacked cisternae that appear to be cemented together by a broad, diffuse electron-dense region (arrowheads).

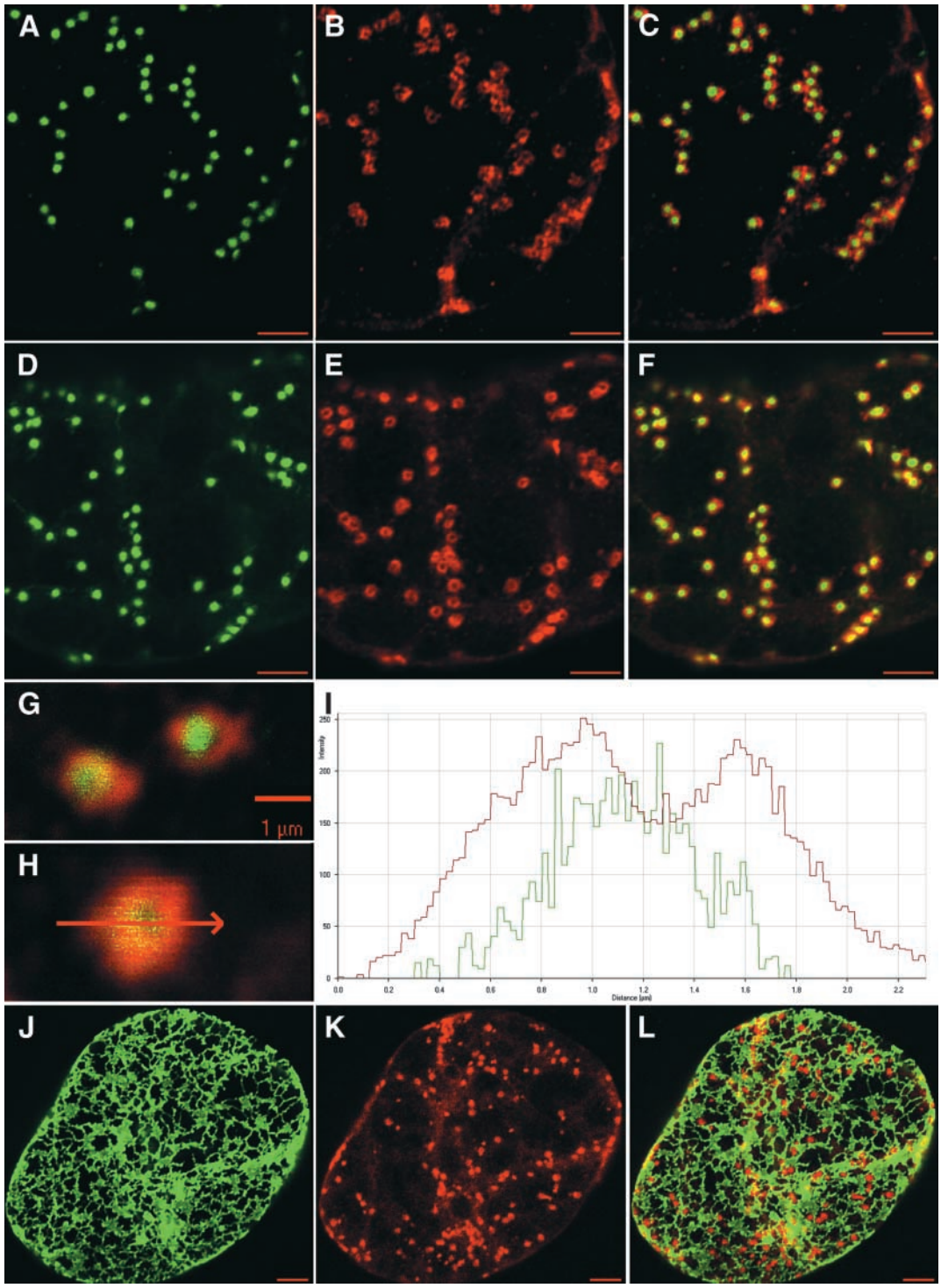

Figure 8. Immunolocalization of γ-COP and Arf1p in GmMan1-GFP and GFP-HDEL BY-2 Cells.

(A) and **(D)** Typical distribution of Golgi stacks in the cortical cytoplasm of GmMan1-GFP cells.
(B) and **(E)** Corresponding immunofluorescence labeling with anti-Atγ-COP and anti-AtArf1p antibodies, respectively.
(C) and **(F)** Composite images obtained after merging **(A)** with **(B)** and **(D)** with **(E)**, respectively.
(G) High magnification of two fluorescent Golgi stacks (green signal, GmMan1-GFP; red signal, Atγ-COP).

DISCUSSION

Recent years have brought enormous progress in our understanding of trafficking in the secretory system of animal and yeast systems (Lippincott-Schwartz et al., 2000; Scales et al., 2000). Similar advances also have been made in the plant kingdom, especially in terms of ER quality control (Vitale and Denecke, 1999) and vacuolar protein sorting (Marty, 1999; Vitale and Raikhel, 1999; Bassham and Raikhel, 2000). From these studies, it has become apparent that most proteins that mediate intracellular membrane traffic in other eukaryotes also are found in plants (Robinson et al., 1998; Sanderfoot et al., 2000; Nebenführ and Staehelin, 2001). Interestingly, despite these similarities at the molecular level, the secretory system in plants is organized differently and performs different functions (Bassham and Raikhel, 2000; Nebenführ and Staehelin, 2001). As we have demonstrated here, these similarities and differences also are reflected in the response of the plant Golgi apparatus to the toxin BFA. Here, we explain how the secondary effects of BFA in plant cells reflect the functional organization of the plant Golgi, and we extrapolate this to all eukaryotic cells.

Initial Site of BFA Action in Plant Cells Is the Golgi Apparatus

One of the first detectable effects of BFA treatment of BY-2 cells is the nearly complete loss of COPI coat proteins (as judged by Atγ-COP and AtArf1) from Golgi stacks, an observation that is identical to that from BFA-treated mammalian cells (Donaldson et al., 1990; Scheel et al., 1997). In addition, the first BFA-related morphological changes detected in both BY-2 (this study) and animal (Lippincott-Schwartz et al., 1989; Hess et al., 2000) involve the Golgi apparatus. These observations strongly support the conclusion that the initial site of BFA action in plants, as in other eukaryotes, is the Golgi apparatus.

Research on mammalian and yeast cells has firmly established that the molecular target of BFA is an Arf1-specific GEF. This was originally inferred from work performed on membrane fractions in vitro (Donaldson et al., 1992; Helms and Rothman, 1992; Randazzo et al., 1993). It has now been substantiated on purified Arf-GEF (Togawa et al., 1999) and by structural analysis of the BFA binding site on the ARF-GDP-GEF complex (Robineau et al., 2000). It also is supported by the finding that BFA-resistant Chinese hamster ovary (CHO) lines appear to produce an Arf1-type GEF (Melancon et al., 1997). Therefore, wherever Arf1 and its associated GEF are localized is the initial site of BFA action.

BFA-sensitive GEFs are localized to the Golgi apparatus of mammalian cells (Narula et al., 1992; Mansour et al., 1999), as are Arf1p and Arf3p (Stearns et al., 1990; Peters et al., 1995). At least three Arf1p binding sites exist in the mammalian Golgi apparatus: the *trans*-Golgi network, where Arf1p is involved in the recruitment of the AP-1 adaptor complex of clathrin-coated vesicles (Traub et al., 1993; Boman et al., 2000); and the two compartments where COPI-coated vesicles are formed: the *cis*-cisternae (Oprins et al., 1993) and the ER-Golgi intermediate compartment (Griffiths et al., 1995; Martinez-Menarguez et al., 1999). Thus, after BFA treatment, the mammalian Golgi apparatus is capable of neither clathrin-coated nor COPI-coated vesicle formation (Robinson and Kreis, 1992; Scales et al., 2000).

Several lines of evidence strongly support a similar conclusion for plant cells. First, both coatomer and Arf homologs have been identified in plants (Movafeghi et al., 1999) and localized to the budding periphery of Golgi cisternae (Pimpl et al., 2000). Second, a candidate for a plant GEF gene, *GNOM*, has been identified (Busch et al., 1996). Third, in the presence of GTPγS, BFA prevents the recruitment of cytosolic Arf1p and coatomer onto plant membranes in vitro (Pimpl et al., 2000). Finally, we have now demonstrated that BFA causes rapid dissociation of COPI coat proteins in vivo. Clathrin-coated vesicles also are formed at the *trans*-Golgi network of plants (Robinson et al., 1998), and there is strong evidence for their participation in the transport of soluble vacuolar proteins containing an N-terminal propeptide sorting signal (Ahmed et al., 2000). Preliminary evidence for the presence of an AP-1–type adaptor at the *trans*-Golgi network also has been found (S. Holstein, N. Happel, and D.G. Robinson, unpublished data). Although not investigated here, it is

Figure 8. (continued).

(H) High magnification of a single fluorescent Golgi stack (green signal, GmMan1-GFP; red signal, AtArf1p).
(I) Fluorescence profile along the arrow shown in **(H)**. The *y* axis gives the intensity of the GmMan1-GFP signal (green curve) and of the AtArf1p signal (red curve) along the arrow. The *x* axis gives the distance in micrometers.
(J) Typical distribution of the cortical ER in the GFP-HDEL cells.
(K) Corresponding immunofluorescence labeling with anti-Atγ-COP.
(L) Merged images from **(J)** and **(K)**.
All images were obtained by confocal microscopy from single optical sections through the cortical cytoplasm of tobacco BY2 cells. Bars = 5 μm except in **(G)** and **(H)**.

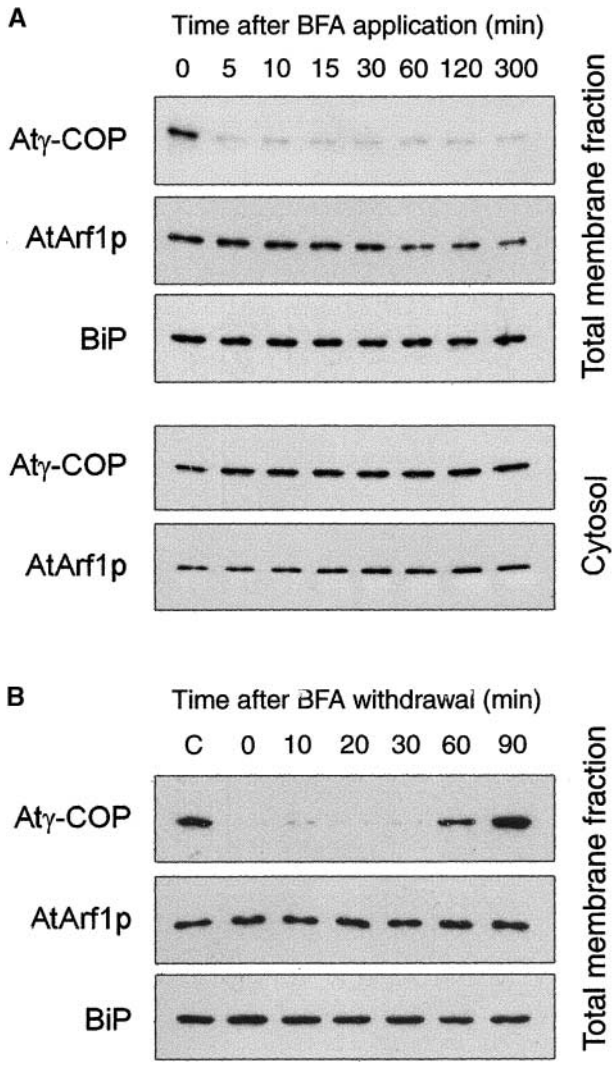

Figure 9. BFA-Induced Release of COPI Coat Proteins and AtArf1p from Tobacco BY-2 Membranes, and Their Reassociation after BFA Removal Analyzed by Protein Gel Blotting.

(A) BY-2 cells were incubated in the presence of 10 μg/mL BFA, and samples were removed at the times indicated. The cells were homogenized and then centrifuged to separate total membranes from the cytosol as described in Methods. Both fractions were probed for gains or losses in coat proteins as indicated. The ER marker BiP was included as a standard lumenal protein.

(B) BY-2 cells were treated with 10 μg/mL BFA for 20 min, washed twice, and then incubated in fresh culture medium. Samples were removed at the times given and processed as in **(A)**. All lanes contained equal amounts of proteins (30 μg). Lane C, untreated control cells.

possible that BFA will block *trans*-Golgi network–based clathrin-coated vesicle formation in plants as well. Therefore, the net effect of BFA on the plant Golgi will be to prevent COPI- and possibly clathrin-mediated vesicle formation and thereby disrupt membrane trafficking within and from the Golgi.

BFA-Induced Rapid Changes in Golgi Morphology Provide Support for the Cisternal Progression Model

The first morphological changes of Golgi stacks in BY-2 cells caused by the addition of BFA are the apparent loss of *cis*-cisternae (Figure 3B) and the redistribution of GmMan1-GFP into the cisternal margins (i.e., the formation of fluorescent doughnuts) (Figure 2B). These secondary changes, which follow the primary effect of GEF inactivation, appear to occur simultaneously and may reflect different facets of the same event. The stunning conclusion from these observations is that the reporter protein GmMan1-GFP, which normally is localized to the *cis* half of BY-2 Golgi stacks (Nebenführ et al., 1999), is still present in Golgi stacks after they have lost identifiable *cis*-cisternae. This raises the question of how a *cis*-Golgi marker can reach the later Golgi compartments in the absence of vesicular transport. One possible explanation is that GmMan1-GFP is always present at low levels in the medial and *trans*-Golgi and that the loss of the bulk of GmMan1-GFP from the Golgi apparatus together with the *cis*-cisternae simply reveals this relatively small population. This, however, would be accompanied by a drastic reduction in fluorescence intensity as the stacks lose their *cis*-cisternae. We have never observed such a reduction in Golgi stack fluorescence during the first 10 min of BFA treatment. In other words, the vast majority of the GmMan1-GFP reporter proteins is still present in individual Golgi stacks at a time when virtually all cisternae with a typical *cis* staining pattern have disappeared.

A more likely explanation for the presence of a *cis*-Golgi protein in *trans*-like cisternae is that the *cis*-cisternae, which are present at the beginning of the BFA treatment, continue to mature in the presence of the drug and thereby change their appearance in electron microscopic sections to that of medial and/or *trans*-cisternae. This maturation may involve the action of a vacuolar H^+-ATPase, which acidifies the cisternal lumen and leads to its osmotic collapse (Griffing and Ray, 1985), by the accumulation of Golgi products such as polysaccharides (Zhang and Staehelin, 1992) or by enzymes that modify membrane lipids (van Meer, 1998). Thus, the morphological characterization of these cisternae as "medial" or "*trans*" may not reflect their composition in terms of Golgi enzymes but instead may indicate BFA-independent changes in membrane composition, lumenal pH, and/or products. The Golgi cisternae remaining after 5 min of BFA treatment, therefore, should be referred to as "*trans*-like cisternae" to indicate both their morphology and their unusual composition.

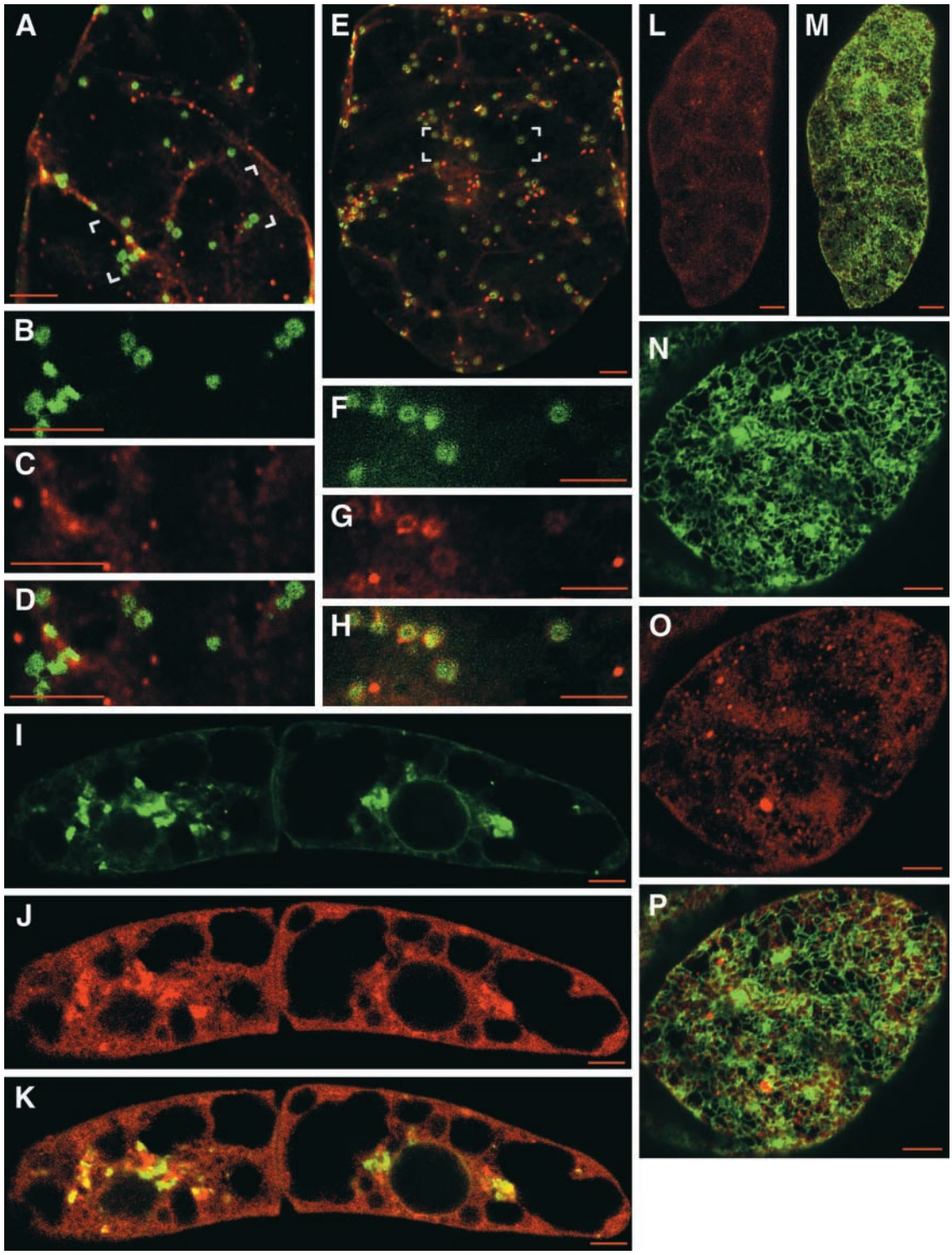

Figure 10. Loss of Atγ-COP and AtArf1p from BY-2 Golgi Stacks.

(A) to **(H)** Cortical cytoplasm of two GmMan1-GFP cells at 5 min after BFA treatment.
(A) Fluorescent double labeling showing the intracellular distribution of GmMan1-GFP (green signal) and Atγ-COP labeling (red signal).
(B) to **(D)** High magnification views of the boxed region in **(A)**.

Normally, the GmMan1-GFP reporter proteins should be recycled from these maturing cisternae to earlier compartments, although based on our previous observations (Nebenführ et al., 1999) a minor portion of this construct seems to exit the Golgi into multivesicular bodies that presumably are destined for degradation. However, neither of these possibilities can occur in the presence of BFA, because of the loss of COPI-coated retrograde transport vesicles and the probable incapacity of the *trans*-Golgi network to produce clathrin-coated vesicles. We assume that under these conditions, the *cis* proteins become displaced to the periphery of the maturing cisternae, where recycling vesicles normally would form. This redistribution of *cis*-type proteins to the rim regions of the *trans*-like cisternae then results in the observed change of Golgi morphology in the fluorescence microscope from small discs to doughnuts of slightly larger diameter. Thus, the presence of the *cis*-Golgi marker GmMan1-GFP in *trans*-like cisternae after 5 to 10 min of BFA treatment can best be explained by assuming that the cisternae gradually mature as they move toward the *trans* side of the stack. Our observations, therefore, are highly pertinent to the current controversy surrounding the mechanism for intra-Golgi transport (for reviews, see Glick, 2000; Griffiths, 2000; Pelham and Rothman, 2000). Although evidence in support of anterograde vesicle traffic in the mammalian Golgi apparatus continues to be published (Brugger et al., 2000; Orci et al., 2000a, 2000b; Volchuk et al., 2000), recent data relating to the intra-Golgi transport of condensed protein aggregates from both animal and plant cells (Bonfanti et al., 1998; Hillmer et al., 2001), as well as older observations on scale-producing algae (Becker and Melkonian, 1996), strongly favor a cisternal progression/maturation model for protein transport in the anterograde direction through the Golgi stack. Our data on the early effects of BFA on Golgi morphology and the distribution of a *cis*-Golgi marker add additional weight to this model.

BFA Blocks the Assembly of New *cis*-Cisternae but Not Vesicle-Mediated Export from the ER

Our interpretation of BFA effects in terms of cisternal maturation suggests that the reduction in the number of Golgi cisternae results from a combination of continued shedding of cisternae at the *trans* side and a simultaneous lack of formation of new cisternae at the *cis* side. This latter point at first seems consistent with the notion that BFA inhibits protein export from the ER, as described originally by Klausner et al. (1992) and expressed more recently in the plant literature (Mullen et al., 1999; Pagny et al., 2000). However, we have shown here that the initial site of BFA action is at the Golgi and that during the time in which severe structural changes are induced in this organelle, there is no visible alteration in ER morphology. It is not immediately obvious how a block of vesicle formation at the Golgi should affect the export capacity of the ER on such a short time scale. In fact, there is no evidence that vesicle formation at the ER ever stops in the presence of BFA. On the contrary, it has been found that mammalian cells are capable of exporting proteins from the ER to the ER-Golgi intermediate compartment even after a 30-min BFA treatment (Füllekrug et al., 1997), at which time the Golgi apparatus has already fused with the ER. In this respect, on occasion we have observed coated budding structures on the ER after 30 min of BFA treatment and even on the ER-Golgi hybrid compartment as late as 5 hr into BFA treatment (Figures 5C and 5D). Thus, it seems likely that export from the ER never stops completely in the presence of the drug, although it may be reduced after the formation of the ER-Golgi hybrid compartment (see below).

The assumption that ER export still occurs during the early minutes of BFA treatment raises the question of why new cisternae cannot form at the *cis* side of Golgi stacks in the presence of BFA. The cisternal progression/maturation model predicts that new *cis*-Golgi cisternae are formed by a

Figure 10. (continued).

(B) GmMan1-GFP signal. Several Golgi stacks show the typical BFA-induced ring-like structure.
(C) Corresponding diffuse Atγ-COP labeling signal.
(D) Merged image. Atγ-COP labeling has almost completely disappeared from the periphery of the Golgi stacks.
(E) Fluorescent double labeling showing the intracellular distribution of GmMan1-GFP (green signal) and AtArf1p labeling (red signal).
(F) to **(H)** High magnification views of the boxed region in **(E)**.
(F) GmMan1-GFP signal. Several Golgi appear as ring-like structures.
(G) Corresponding AtArf1p labeling signal. The intensity of the labeling is weak, but ring-shaped halos still can be visualized.
(H) Merged image. The Atγ-COP halos are found at the periphery of most doughnut-shaped GmMan1-GFP signals.
(I) Perinuclear GmMan1-GFP pleiomorphic aggregates after 20 min of BFA treatment.
(J) Corresponding AtArf1p labeling. The signal is diffuse throughout the cytoplasm of the cells and sometimes is concentrated in the vicinity of the nucleus.
(K) By merging **(I)** and **(J)**, AtArf1p labeling often was found to be distinct from the GmMan1-GFP pleiomorphic aggregates.
(L) to **(P)** Cortical cytoplasm of two GFP-HDEL cells 20 min after BFA treatment showing diffuse Atγ-COP **(L)** and AtArf1p labeling **(O)** together with unchanged GFP-HDEL fluorescence distribution **(N)**. Compare untreated cells (Figure 8J). **(M)** and **(P)** show merged images.
All images were obtained by confocal microscopy from single optical sections of tobacco GmMan1-GFP or GFP-HDEL cells. Bars = 5 μm.

combination of newly produced anterograde ER-to-Golgi (COPII) vesicles and recycling retrograde intra-Golgi (COPI) vesicles. In BFA-treated cells, the population of retrograde transport vesicles is missing, because their budding at older Golgi cisternae is inhibited. This imbalance in the vesicle population may make it impossible for the anterograde vesicles to assemble into a stable cisterna on the *cis* side of the stack. In our experiments, we observed that a small percentage of stacks still contained small *cis*-like cisternae after 5 to 10 min in BFA (data not shown), which may reflect this continued arrival of ER-to-Golgi transport vesicles. However, these cisternae never reached their full size and disappeared from the Golgi stack remnants over time.

Different Responses of Plant and Mammalian Golgi to BFA Reflect Underlying Differences in Architecture and Functional Organization

As documented in this article, the effects of BFA on Golgi morphology in BY-2 cells are very different from those reported for mammalian cells. Light microscopic studies of mammalian cells have shown that BFA induces the formation of membrane tubules that emanate from the perinuclear Golgi complex and extend into the cell periphery before the Golgi membranes are absorbed into the ER (Sciaky et al., 1997). A recent detailed study of cryofixed human hepatoma cells has further demonstrated that, unlike plant Golgi stacks, animal Golgi rapidly ($<$2 min) lose their structural integrity during BFA treatment (Hess et al., 2000). This breakdown of Golgi organization is manifested in a loss of stacking and an extensive tubulation of the cisternae, which initially do not fuse with the ER (Hess et al., 2000), two effects not shown by BY-2 cells and that have never been described in the plant literature. Although the rapidity of the response of the hepatoma cells to BFA could be related to permeability and/or temperature of incubation, the radically different morphological responses to BFA most likely result from the different functional architecture of the two Golgi systems. Plant Golgi stacks are relatively small units that can move actively through the cytoplasm along actin filaments, a property that requires strong cohesive forces to maintain stack integrity (Nebenführ et al., 1999; also see below). In contrast, the mammalian Golgi complex is a large organelle whose perinuclear organization is dependent on the presence of microtubules emanating from the centrioles (Burkhardt, 1998). In such cells, transport to and from the Golgi also occurs along microtubules (Toomre et al., 1999). Thus, the BFA-induced formation of Golgi tubules in mammalian cells may reflect the continued transport of membrane-associated Golgi products to the cell periphery despite the inability of the Golgi to package them into vesicles. Plant cells do not appear to use either of these mechanisms (Nebenführ and Staehelin, 2001) and consequently maintain an almost normal appearance of Golgi cisternae until these fuse with the ER. Therefore, the different effects of BFA on Golgi morphology in plants and mammals are likely caused by the structural adaptations of this organelle to the different functional requirements of these organisms.

Formation of BFA-Induced ER-Golgi Hybrid Stacks Results from the Fusion of ER Cisternae with Stacked Golgi Cisternae

The initial loss of cisternae from Golgi stacks in BFA-treated cells is followed by the appearance of ER-Golgi hybrid stacks, which have ER cisternae associated first with one side of the Golgi stack and then with both, and ultimately with all cisternae in the stack being continuous with the ER. The presence of stacked ER regions in BFA-treated BY-2 cells was first reported by Yasuhara et al. (1995), but those authors did not suggest how these structures might have formed. We propose that the formation of these hybrid stacks is caused by the fusion of ER with individual Golgi cisternae, followed by a mixing of membrane components that results in the ER-like appearance of the fused cisterna (Figure 12).

The fusion of ER and Golgi membranes is likely to be mediated by the SNARE molecules present in the Golgi cisternae, which normally would mediate the fusion of retrograde Golgi-to-ER transport vesicles with their target organelle (Elazar et al., 1994). The BFA-induced block of COPI coat formation leaves these SNARE molecules exposed at the periphery of the Golgi cisternae and free to fuse with their counterparts in ER membranes that make contact with Golgi cisternae. Interestingly, we have never observed any distinct structural intermediates that depict this fusion event, despite the very different staining characteristics of the two membranes. This implies that the mixing of membrane components after fusion must be very rapid, consistent with the reported high diffusional mobility of Golgi proteins and lipids (Cole et al., 1996; Zaal et al., 1999) and the postulated difference in free energy level of Golgi and ER membranes (Sciaky et al., 1997).

An important implication of these findings is that although the general intermixing of the cisternal membranes is very fast, the molecules that maintain Golgi membrane stacking in tobacco BY-2 cells do not participate in this initial mixing event. In other words, the membrane adhesion forces that keep plant Golgi stacks intact during their movement through the cytoplasm (Boevink et al., 1998; Nebenführ et al., 1999) must be very strong compared with those of mammalian cells (Sciaky et al., 1997) and be able to resist the membrane-mixing forces. A morphological manifestation of these cohesive forces in BY-2 cell Golgi stacks are the intercisternal filaments, which are present between medial and *trans*-cisternae in untreated cells and between all cisternae in Golgi stacks remaining after 10 or more min in BFA-treated cells (Figure 3). These intercisternal filaments are thought to form physical links between adjacent cisternae and to serve as anchoring sites for Golgi enzymes (Staehelin

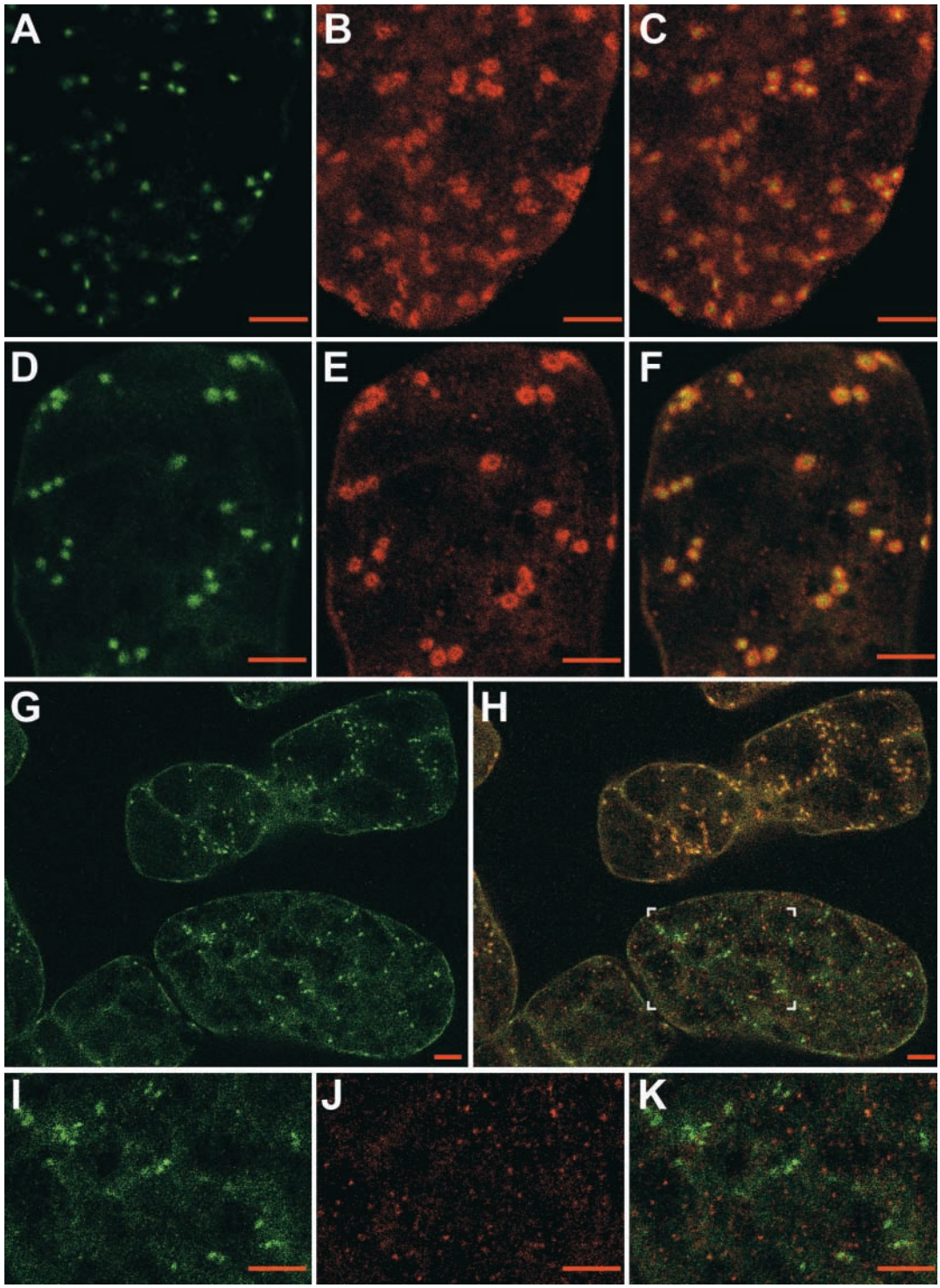

Figure 11. Recovery of Golgi Morphology and Arf Labeling.

(A) and **(D)** Fluorescent spots typical of the distribution of Golgi stacks in BY-2 cells expressing GmMan1-GFP at 2 hr after removal of BFA.
(B) and **(E)** Immunolocalization of Atγ-COP and AtArf1p, respectively.
(C) and **(F)** Corresponding merged images.
Immunofluorescence labeling was very similar to that observed in nontreated cells (cf. with Figures 8A to 8F).

et al., 1990). The fact that these structures are very prominent in BY-2 cells (Figure 3A) and root cap cells (Figure 6C) may explain why the ER-Golgi hybrid cisternae remain associated with the stacks. In a number of instances, we have observed intercisternal filaments between Golgi cisternae and adjacent ER-Golgi hybrid membranes (Figure 3F), which again highlights how these hybrid stacks are formed and what holds them together. Together, these findings suggest that ER-Golgi hybrid stacks can arise only in cells containing Golgi stacks with strong intercisternal bonds (i.e., Golgi stacks whose cisternae are connected by numerous intercisternal filaments). In this regard, we note that Golgi stacks in pollen tubes appear to have very few intercisternal filaments and that treatment with BFA leads to their rapid disappearance (Rutten and Knuiman, 1993). Our prediction could be tested by carefully examining the effects of BFA in tissues that do not display prominent intercisternal filaments, such as meristems (Staehelin et al., 1990).

The progressive appearance of ER-Golgi hybrid stacks, which was first observed ~10 min after the start of treatment, coincided with the gradual loss of Golgi stacks in fluorescence images and with the appearance of the ER-like fluorescent network. This temporal correlation of the three events observed at the both the electron and light microscopic levels suggests that they are manifestations of the same event, namely, the fusion of Golgi cisternae with the ER and the redistribution of Golgi proteins into a novel ER-Golgi hybrid compartment. This process occurred at different times for the individual Golgi stacks during a period of ~15 min. This BFA-induced redistribution of a *cis*-Golgi marker into the ER in BY-2 cells is similar to the redistribution of a *trans*-Golgi marker described for tobacco mesophyll cells and Arabidopsis protoplasts (Boevink et al., 1998; Kim et al., 2001). In both cases, the loss of fluorescent Golgi stacks was accompanied by an increase in ER-like fluorescence, thus highlighting the formation of an ER-Golgi hybrid compartment. However, it is important to note that the "retrograde transport of Golgi membrane protein into the ER in response to BFA" (Boevink et al., 1998) is brought about by the wholesale fusion of entire Golgi cisternae with the ER and not by vesicle-mediated carriers that occur in untreated cells.

Variability in Responses to BFA May Reflect Differences in the Physiological Status of the Golgi Apparatus

Throughout our experiments, we noticed a certain degree of variability in the morphological responses of individual Golgi stacks to BFA treatment. Although all stacks appeared to lose their associated COPI coat proteins within the first 5 min of treatment, the rate at which they proceeded through the subsequent morphological changes differed from cell to cell and to a lesser extent even from stack to stack within a given cell. One example is the gradual disappearance of fluorescent Golgi stacks within a cell, which suggests that the fusion of the ER to the last remaining Golgi cisterna in a stack is not synchronous. A more striking example is the retention of clusters of small Golgi remnants together with numerous Golgi-derived vesicles in the perinuclear region. These structures often are referred to as BFA compartments and have been observed in a number of plant cell types (Satiat-Jeunemaitre et al., 1996). We believe that the presence of these BFA compartments in a subset of BY-2 cells indicates an important mechanistic explanation for their formation that may resolve some of the long-standing disputes in the plant literature.

As discussed above, the fusion of ER and Golgi membranes caused by BFA most likely is mediated by the interaction of SNARE molecules in the two membranes. Thus, the availability of these SNARE molecules at the Golgi should affect the rate at which the fusion occurs and, therefore, how fast distinct Golgi stacks disappear. SNARE availability is likely nfluenced by two parameters: (1) the number of SNARE molecules present in a given Golgi stack before BFA treatment; and (2) the fraction of COPI coat proteins still associated with the Golgi membranes at sites where they can occlude Golgi SNAREs and prevent them from interacting with their ER partners. The first parameter probably reflects the rate of membrane recycling in a stack, which may differ from tissue to tissue depending on the products being formed (glycoproteins versus polysaccharides) or at different stages of the cell cycle (Noguchi and Watanabe, 1999). The second parameter reflects the effectiveness of BFA in preventing COPI coat recruitment and depends on the sensitivity of the cell type under investigation and the BFA concentration used. We believe that at least some of the

Figure 11. (continued).

(G) GmMan1-GFP fluorescence in BY-2 cells at 1 hr after removal of BFA.

(H) Same cells as in **(G)** but as merged image with AtArf1p labeling. The cells at the top present nearly normal Golgi-associated AtArf1p labeling, whereas in the cells at the bottom, almost only diffuse AtArf1p labeling is seen.

(I) to **(K)** The boxed region in **(H)** at higher magnification.

(I) Intracellular distribution of GmMan1-GFP.

(J) AtArf1p labeling.

(K) Corresponding merged image. AtArf1p fluorescence is dispersed throughout the cortical cytoplasm.

All images were obtained by confocal microscopy from single optical sections through the cortical cytoplasm of BY-2 cells expressing GmMan1-GFP. Cells were first treated for 20 min with BFA and then incubated for 1 to 2 hr in growth medium before fixation and immunofluorescence. Bars = 5 μm.

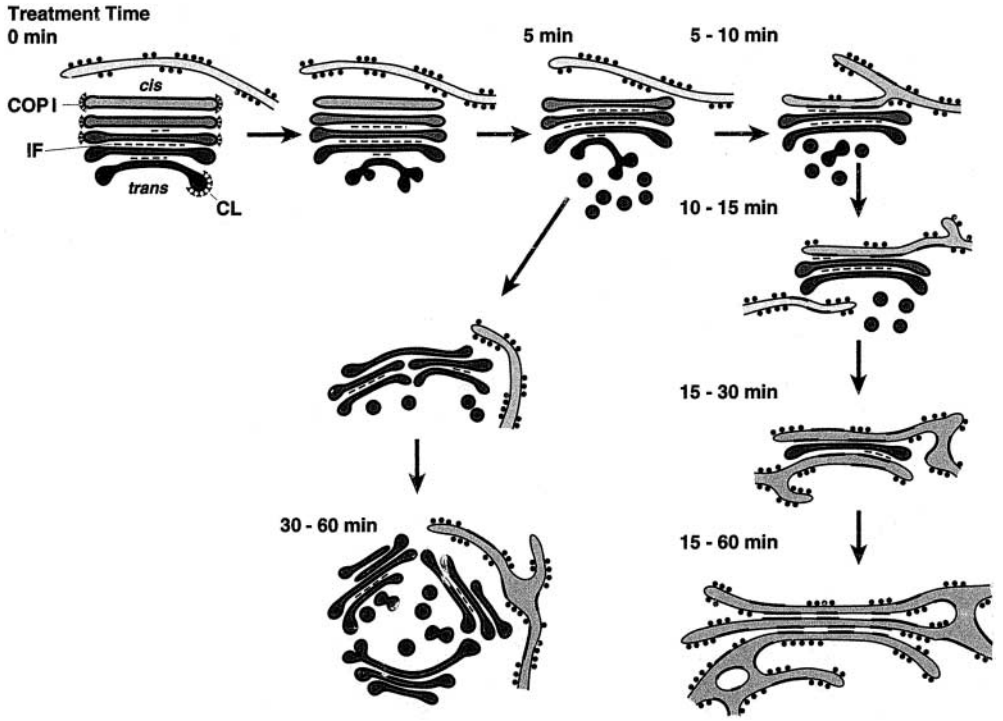

Figure 12. Early BFA Effects on Tobacco BY-2 Suspension-Cultured Cells.

The first effect of the toxin we have visualized with our tools is the loss of COPI coats from the Golgi. This is followed by a loss of the oldest, *trans*-most (*trans*-Golgi network) cisterna and the simultaneous maturation of the younger cisternae, consistent with the cisternal progression/maturation model of intra-Golgi trafficking. After ~10 min, ER begins to fuse to individual cisternae in the stack, presumably starting with the youngest cisterna. This is followed by ER-to-Golgi fusion at the opposite pole of the stack, and eventually with all cisternae in the stack, resulting in a region of stacked ER that contains patches of Golgi proteins (right branch). Some stacks never fuse with the ER and instead become clustered in the perinuclear region, where they form so-called BFA compartments (left branch). Note that the times indicated are representative only for those stacks that go through this process slowly. Many stacks appear to undergo these transformations much more quickly and become absorbed completely into the ER system without forming distinct stacked ER-Golgi hybrids.
IF, intercisternal filaments; CL, clathrin.

variation in BFA responses described in the plant literature can be explained in terms of these parameters and their effects on the rate of ER-to-Golgi fusion.

The apparent BFA-induced loss of *cis*-Golgi cisternae described here also has been recorded elsewhere in other organisms (Dairman et al., 1995; Salomon and Meindl, 1996; Robinson et al., 1997) and in suspension-cultured sycamore cells when a more potent form of BFA (7-dehydrobrefeldin A) was applied (Driouich et al., 1997). Interestingly, clear evidence for the formation of BFA-induced ER-Golgi hybrid compartments in plant cells has been obtained in only a few cell types (Rutten and Knuiman, 1993; Kaneko et al., 1994; Yasuhara et al., 1995; Boevink et al., 1998; Kim et al., 2001). It is possible that the fusion of Golgi membranes with the ER simply was not detected in other systems because appropriate markers were not available. A case in point is the monoclonal antibody JIM84, a commonly used marker for Golgi stacks in plants (Horsley et al., 1993). This, and an antibody directed against plant Lewis antigen, recognizes a complex carbohydrate epitope that is generated very late in the Golgi (Fitchette et al., 1999). According to our interpretation of BFA effects in plant cells (Figure 12), we would predict that the oldest, or *trans*-most, parts of Golgi stacks are lost through sloughing at the beginning of BFA treatment and are no longer available for fusion with the ER. This would reduce the amount of a potential *trans* marker available for redistribution and is consistent with published reports that the JIM84 epitope is never found in the ER during BFA treatment (Satiat-Jeunemaitre and Hawes, 1992).

Long-Term Treatment of Plant Cells with BFA Results in a Pathological Morphology of the ER-Golgi Hybrid Compartment

Although the ER-Golgi hybrid compartment that resulted from the fusion of ER with Golgi cisternae initially displayed a typical ER morphology, we noticed several unusual fea-

tures that became more prominent as time progressed. These included membranes that exhibited either an unusually straight morphology or displayed wide, smoothly curved domains (Figure 7), two characteristics that indicate an increased stiffness of the membranes compared with the ER in untreated cells. This increased stiffness may have resulted from the presence of patches of Golgi proteins that usually associate laterally in the flattened cisternae of the Golgi. Consistent with this interpretation is the observed increase in ribosome-free regions on the ER-Golgi hybrid membranes. Another unusual feature of the ER-Golgi hybrid compartment that results from prolonged exposure to BFA is the accumulation of electron-dense material in its dilated lumen. This may be explained by the gradual reduction in export from the ER despite ongoing translational activity plus the presence of resorbed Golgi enzymes. The continued activity of Golgi enzymes in the ER-Golgi hybrid has been demonstrated previously by the presence of typical Golgi-type modifications of the oligosaccharides on ER-resident glycoproteins, which occurred only after incubation of the cells with BFA (Crofts et al., 1999; Pagny et al., 2000).

Similar changes in the morphology of the ER as a result of long-term BFA treatment have been described previously for a variety of plant cell types preserved by chemical fixation methods (Kimura et al., 1993; Schindler et al., 1994; Kunze et al., 1995; Satiat-Jeunemaitre et al., 1996). These ultrastructural changes in ER-Golgi hybrid morphology were accompanied by a dramatic reorganization of this novel organelle, resulting in a highly abnormal distribution of GFP fluorescence that did not resemble the typical ER organization of untreated BY-2 cells (Figure 7A). A similar global restructuring of the ER has been described in BFA-treated root cells of maize (Henderson et al., 1994; Satiat-Jeunemaitre et al., 1996). Together, these results clearly indicate that exposure of BY-2 cells, and probably all plant cells, to BFA for periods of >30 to 60 min results in highly pathological changes of the endomembrane system of these cells. This puts into question the physiological competence of the cells and thus represents a major caveat for all studies that use lengthy (>1 hr) treatments with BFA.

Conclusions

In summary, the treatment of tobacco BY-2 suspension-cultured cells with BFA results in a series of events that lead to the disappearance of a distinct Golgi apparatus and to the complete disruption of the secretory system. The first effect of the toxin we have visualized with our tools is the loss of COPI coats from the Golgi and hence the disruption of vesicle formation at this organelle. Although this initial response appears to be the same in all eukaryotic cells studied to date, the secondary effects that lead to the physical disruption of the Golgi apparatus differ between plant and animal cells, reflecting the underlying specific structural and functional adaptations of this organelle to the requirements of the secretory system in different organisms. These adaptations, most notably the increased mechanical stability of plant Golgi stacks, have allowed us to study the sequence of events that occur in response to BFA in great detail and to conclude that intra-Golgi transport occurs by cisternal progression/maturation and that fusion of the ER with Golgi cisternae is responsible for the loss of Golgi stacks from the cells.

METHODS

Materials

Tobacco (*Nicotiana tabacum* var Bright Yellow 2 [BY-2]) was cultivated in the dark by shaking (120 rpm) in suspension at 27°C using either Murashige and Skoog (1962) medium or a modified Linsmaier and Skoog (1965) medium. Cells were maintained in the log phase by subculturing weekly into fresh medium at a dilution of 1:50. Three different cell lines were used: (1) wild-type cells (obtained from Dr. Y. Moriyasu, Shizuoka University, Japan); (2) cells transformed with an α-mannosidase 1–green fluorescent protein fusion construct (Man1-GFP) that localizes predominantly to the *cis*-Golgi (Nebenführ et al., 1999); and (3) cells transformed with a GFP-HDEL fusion construct that remains in the lumen of the endoplasmic reticulum (ER) (Nebenführ et al., 2000).

Individual surface-sterilized, water-washed tobacco seed (var SR1 Petit Havana) were allowed to germinate under sterile conditions (7 days at 27°C; 15-hr-weak-light/9-hr-dark cycles) in the wells of a microtiter plate containing 1 mL of Murashige and Skoog medium.

Antibodies

The antibodies used were the same as those used in previous investigations (Movafeghi et al., 1999; Pimpl et al., 2000), applied at the following primary dilutions (for protein gel blotting/for confocal laser scanning microscopy studies): Atγ-COP, 1:2500/1:1000; AtArf1p, 1:2500/1:1000; and BiP, 1:10,000.

Brefeldin A Treatment and Recovery

Stock solutions of brefeldin A (BFA; Molecular Probes Europe, Leiden, The Netherlands) were prepared by dissolving 5 mg of BFA in 1 mL of DMSO. Aliquots of this stock solution were added to 3- to 4-day-old suspension cultures to give a final concentration of 10 μg/mL (35.7 mM). Incubation occurred for various periods under continuous agitation. Controls containing equivalent concentration of DMSO did not show any response to the solvent. BFA-treated cells were removed from the cultures at the times indicated in the appropriate figure legends and either fixed directly for immunofluorescence or harvested by low-speed centrifugation (in the case of electron microscopy) or vacuum filtration onto nitrocellulose filters (for biochemical analysis). Specimens for electron microscopy were processed immediately; the cells collected on nitrocellulose filters were frozen in liquid nitrogen until further use. Root tips (1 mm) from intact tobacco seedlings, exposed to BFA at final concentrations of 50 or 100 μg/mL, were excised and immediately fixed for electron

microscopy. For recovery experiments, BY-2 cells were treated with 10 μg/mL BFA for 20 min and then sedimented by low-speed centrifugation and resuspended in fresh (BFA-free) culture medium. After a second wash cycle of sedimentation and resuspension, the cells were returned to the shaker under normal growth conditions. Samples were removed at the times indicated in Figure 9, harvested, and processed as described above.

Immunofluorescence Labeling

BY-2 cells 3 to 4 days after subculture were fixed with 1% glutaraldehyde in culture medium for 15 min at room temperature under gentle agitation. After two washes in culture medium, cells were treated with 0.1% (w/v) Pectolyase Y23 (Kikkoman Corp., Tokyo, Japan) and 1% (w/v) Cellulase RS (Onozuka; Yakult Honsha Corp., Tokyo, Japan) for 1 hr at 28°C to partially digest cell walls, washed three times in PBS, and finally transferred to 10 mL of freshly prepared PBS containing 0.1% (w/v) $NaBH_4$. After overnight incubation at 4°C to permeabilize cells and reduce autofluorescence, cells were allowed to settle onto poly-L-lysine–coated cover slips before the addition of blocking solution consisting of PBS, 5% (w/v) BSA, 5% (v/v) normal goat serum, and 0.1% (v/v) cold water fish skin gelatin (Aurion, Wageningen, The Netherlands) for 1 hr at room temperature. Cells then were incubated at 4°C overnight in a 1:1000 dilution of the primary antibody in PBS plus 0.1% (v/v) acetylated BSA (Aurion), washed four times in PBS, and incubated again in the dark for 4 hr at room temperature with Alexa-fluor 568 goat anti-rabbit immunoglobulin G (Molecular Probes Europe) diluted 1:300 in PBS plus 0.1% (v/v) acetylated BSA. Cells were washed again four times before observation. Control experiments in which primary antibodies were omitted were performed each time to verify the specificity of the labeling.

Confocal Laser Scanning Microscopy

Before observation, fixed cells were mounted in a chamber containing PBS and 0.1% (w/v) Na ascorbate, pH 7.4, to reduce photobleaching. Observation of living cells was performed in a perfusion chamber with a continuous supply of fresh medium at a flow rate of 0.5 mL/min. Cells were observed with a Zeiss (Jena, Germany) LSM510 laser scanning confocal microscope equipped with an inverted Zeiss Axiovert 100M microscope and a ×63, 1.2 numerical aperture water immersion objective. Laser scanning was performed using the multitrack mode to avoid bleed through. Unless stated otherwise, optical sections were 0.45 μm thick. Excitation and emission wavelengths were 488 and 505 to 545 nm for GFP and 543 and 560 nm for Alexa-fluor 568. Image processing occurred in LSM510 version 2.5 (Zeiss) and PhotoShop 5.5 (final image assembly; Adobe Systems, San Jose, CA).

Electron Microscopy

For conventional electron microscopy, cells were fixed immersed in 1 mL of a primary fixative containing 2% (v/v) glutaraldehyde and 0.1 mL of saturated picric acid in 25 mM potassium phosphate, pH 7.4, for 15 min at room temperature before transferring to 4°C for 16 hr. After four washes in 25 mM Pipes, pH 7.0, at room temperature, the cells were transferred to a secondary fixative containing 2% (w/v) osmium tetroxide and 0.5% (w/v) potassium ferrocyanide in 25 mM Pipes, pH 7.0, for 2 hr at room temperature. The cells then were washed twice in 25 mM Pipes, pH 7.0, and twice in distilled water before transferring to 2% (w/v) aqueous uranyl acetate for 16 hr at 4°C. After washing twice in water, the cells were dehydrated in an acetone series and embedded in Spurr's resin.

Sample processing for high-pressure freezing followed a published procedure (Samuels et al., 1995). Briefly, after low-speed centrifugation, cells were resuspended in 25% dextran as a cryoprotectant, concentrated on a nylon mesh, and immediately frozen in an HPM010 high-pressure freezer (Bal-Tec, Balzers, Lichtenstein). Frozen cells were transferred under liquid nitrogen into cryovials containing 0.5% glutaraldehyde and 0.1% tannic acid in anhydrous acetone. Freeze substitution was performed on dry ice (−80°C) for 4 days, after which samples were washed three times with anhydrous acetone (at −80°C) and transferred to 2% osmium tetroxide in acetone. After an additional 1 day on dry ice, samples were slowly warmed to −20°C for 20 hr, to 4°C for 24 hr, and to room temperature for 6 hr. After several rinses in anhydrous acetone, cell pellets were removed from the sample holders and embedded in epoxy resin (Epon 812, Agar Scientific Limited, Stansted, UK). Ultrathin sections (40 to 60 nm) from both conventionally and high-pressure fixed samples were cut on a Leica (Wetzlar, Germany) Ultracut microtome and stained with methanolic uranyl acetate (2%) and Reynold's lead citrate. Ultrastructural observations were performed with an electron microscope (CM10; Philips, Eindhoven, The Netherlands) operating at 80 kV.

Preparation of Total Membrane and Cytosol Fractions

Frozen cells on nitrocellulose filters were ground to a fine powder in liquid nitrogen and then taken up in 10 mL of a homogenization medium containing 25 mM Hepes/KOH, pH 7.5, 300 mM sucrose, 1 mM DTT, 2 mM *o*-phenanthroline, 1.4 μg/L pepstatin, 0.5 μg/L leupeptin, 2 μg/L aprotinin, and 1 μg/L *trans*-epoxysuccinyl-L-leucylamido-(4-guanido)-butane. After filtering through one layer of Miracloth (Calbiochem) and two layers of gauze, the homogenate was centrifuged at 5000*g* for 15 min. The supernatant then was centrifuged at 100,000*g* for 1 hr to separate total membranes (pellet) from the cytosol (supernatant). Proteins in both fractions were precipitated out using the chloroform/methanol procedure of Wessel and Flügge (1984).

Gel Electrophoresis, Protein Gel Blotting, and Protein Determination

All procedures were performed exactly as described previously (Pimpl et al., 2000).

ACKNOWLEDGMENTS

We thank Dorothea Dasbach and Stefanie Gold for technical assistance. Financial support from the Deutsche Forschungsgemeinschaft (SFB 523), the National Institutes of Health (Grant No. GM18639 to L.A.S.), and the Centre National de la Recherche Scientifique is gratefully acknowledged. The Inter-Institute Confocal Microscopy Plate-Form was cofinanced by the Centre National de la Recherche Scientifique, the Université Louis Pasteur, the Région Alsace, and the Association pour la Recherche sur le Cancer.

Received June 12, 2001; accepted September 24, 2001.

REFERENCES

Ahmed, S.U., Rojo, E., Kovaleva, V., Venkataraman, S., Dombrowski, J.E., Matsuoka, K., and Raikhel, N.V. (2000). The plant vacuolar sorting receptor AtELP is involved in transport of NH_2-terminal propeptide-containing vacuolar proteins in *Arabidopsis thaliana*. J. Cell Biol. **149,** 1335–1344.

Bassham, D.C., and Raikhel, N.V. (2000). Plant cells are not just green yeast. Plant Physiol. **122,** 999–1001.

Batoko, H., Zheng, H.-Q., Hawes, C., and Moore, I. (2000). A Rab1 GTPase is required for transport between the endoplasmic reticulum and Golgi apparatus and for normal Golgi movement in plants. Plant Cell **12,** 2201–2218.

Becker, B., and Melkonian, M. (1996). The secretory pathway of protists: Spatial and functional organization and evolution. Microbiol. Rev. **60,** 697–721.

Boevink, P., Oparka, K., Santa Cruz, S., Martin, B., Betteridge, A., and Hawes, C. (1998). Stacks on tracks: The plant Golgi apparatus traffics on an actin/ER network. Plant J. **15,** 441–447.

Boman, A.L., Zhang, C.-J., Zhu, X., and Hahn, R.A. (2000). A family of ADP-ribosylation factor effectors that can alter membrane transport through the *trans*-Golgi. Mol. Biol. Cell **11,** 1241–1255.

Bonfanti, L., Mironov, A.A., Jr., Martínez-Menárguez, J.A., Martella, O., Fusella, A., Baldassarre, M., Buccione, R., Geuze, H.J., Mironov, A.A., and Luini, A. (1998). Procollagen traverses the Golgi stack without leaving the lumen of cisternae: Evidence for cisternal maturation. Cell **95,** 993–1003.

Brugger, B., Sandhoff, R., Wegehingel, S., Gorgas, K., Malsam, J., Helms, J., Lehmann, W., Nickel, W., and Wieland, F. (2000). Evidence for segregation of sphingomyelin and cholesterol during formation of COPI-coated vesicles. J. Cell Biol. **151,** 507–518.

Burkhardt, J.K. (1998). The role of microtubule-based motor proteins in maintaining the structure and function of the Golgi complex. Biochim. Biophys. Acta **1404,** 113–126.

Busch, M., Mayer, U., and Jurgens, G. (1996). Molecular analysis of the Arabidopsis pattern formation of gene GNOM: Gene structure and intragenic complementation. Mol. Gen. Genet. **250,** 681–691.

Chardin, P., and McCormick, F. (1999). Brefeldin A: The advantage of being uncompetitive. Cell **97,** 153–155.

Chavrier, P., and Goud, B. (1999). The role of ARF and Rab GTPases in membrane transport. Curr. Opin. Cell Biol. **11,** 466–475.

Cole, N.B., Smith, C.L., Sciaky, N., Terasaki, M., Edidin, M., and Lippincott-Schwartz, J. (1996). Diffusional mobility of Golgi proteins in membranes of living cells. Science **273,** 797–801.

Crofts, A.J., Leborgne-Castel, N., Hillmer, S., Robinson, D.G., Phillipson, B., Carlsson, L.E., Ashford, D.A., and Denecke, J. (1999). Saturation of the endoplasmic reticulum retention machinery reveals anterograde bulk flow. Plant Cell **11,** 2233–2247.

Dairman, M., Donofrio, N., and Domozych, D. (1995). The effects of brefeldin A upon the Golgi apparatus of the green algal flagellate *Gleomonas kupfferi*. J. Exp. Bot. **46,** 181–186.

Donaldson, J., Lippincott-Schwartz, J., Bloom, G., Kreis, T., and Klausner, R. (1990). Dissociation of a 110-kD peripheral membrane protein from the Golgi apparatus is an early event in brefeldin A action. J. Cell Biol. **111,** 2295–2306.

Donaldson, J.G., Finazzi, D., and Klausner, R.D. (1992). Brefeldin A inhibits Golgi membrane–catalysed exchange of guanine nucleotide onto ARF protein. Nature **360,** 350–352.

Driouich, A., and Staehelin, L.A. (1997). The plant Golgi apparatus: Structural organization and functional properties. In The Golgi Apparatus, E.G. Berger and J. Roth, eds (Basel, Switzerland: Birkhäuser Verlag), pp. 275–301.

Driouich, A., Faye, L., and Staehelin, L.A. (1993). The plant Golgi apparatus: A factory for complex polysaccharides and glycoproteins. Trends Biochem. Sci. **18,** 210–214.

Driouich, A., Jauneau, A., and Staehelin, L. (1997). 7-Dehydrobrefeldin A, a naturally occurring brefeldin A derivative, inhibits secretion and causes a *cis*-to-*trans* breakdown of Golgi stacks in plant cells. Plant Physiol. **113,** 487–492.

Duden, R., Hosobuchi, M., Hamamoto, S., Winey, M., Byers, B., and Schekman, R. (1994). Yeast β- and β′-coat proteins (COP): Two coatomer subunits essential for endoplasmic reticulum-to-Golgi protein traffic. J. Biol. Chem. **269,** 24486–24495.

Elazar, Z., Orci, L., Ostermann, J., Amherdt, M., Tanigawa, G., and Rothman, J.E. (1994). ADP-ribosylation factor and coatomer couple fusion to vesicle budding. J. Cell Biol. **124,** 415–424.

Fitchette, A., Cabanes-Macheteau, M., Marvin, L., Martin, B., Satiat-Jeunemaitre, B., Gomord, V., Crooks, K., Lerouge, P., Faye, L., and Hawes, C. (1999). Biosynthesis and immunolocalization of Lewis a-containing N-glycans in the plant cell. Plant Physiol. **121,** 333–344.

Fujiwara, T., Oda, K., Yokota, S., Takatsuki, A., and Ikehara, Y. (1988). Brefeldin A causes disassembly of the Golgi complex and accumulation of secretory proteins in the endoplasmic reticulum. J. Biol. Chem. **263,** 18545–18552.

Füllekrug, J., Sonnichsen, B., Schafer, U., van Nguyen, P., Soling, H., and Mieskes, G. (1997). Characterization of brefeldin A induced vesicular structures containing cycling proteins of the intermediate compartment/*cis*-Golgi network. FEBS Lett. **404,** 75–81.

Glick, B.S. (2000). Organization of the Golgi apparatus. Curr. Opin. Cell Biol. **12,** 450–456.

Gomez, L., and Chrispeels, M. (1993). Tonoplast and soluble vacuolar proteins are targeted by different mechanisms. Plant Cell **5,** 1113–1124.

Griffing, L., and Ray, P. (1985). Involvement of monovalent cations in Golgi secretion by plant cells. Eur. J. Cell Biol. **36,** 24–31.

Griffiths, G. (2000). Gut thoughts on the Golgi complex. Traffic **1,** 738–745.

Griffiths, G., Pepperkok, R., Locker, J.K., and Kreis, T.E. (1995). Immunocytochemical localization of β-COP to the ER-Golgi boundary and the TGN. J. Cell Sci. **108,** 2839–2856.

Harter, C. (1999). COPI proteins: A model for their role in vesicle budding. Protoplasma **207,** 125–132.

Helms, J.B., and Rothman, J.E. (1992). Inhibition by brefeldin A of a Golgi membrane enzyme that catalyses exchange of guanine nucleotide bound to ARF. Nature **360,** 352–354.

Henderson, J., Satiat-Jeunemaitre, B., Napier, R., and Hawes, C. (1994). Brefeldin A–induced disassembly of the Golgi apparatus is

followed by the disruption of the endoplasmic reticulum in plant cells. J. Exp. Bot. **45,** 1347–1351.

Hess, M., Muller, M., Debbage, P., Vetterlein, M., and Pavelka, M. (2000). Cryopreparation provides new insight into the effects of brefeldin A on the structure of the HepG2 Golgi apparatus. J. Struct. Biol. **130,** 63–72.

Hillmer, S., Movafeghi, A., Robinson, D.G., and Hinz, G. (2001). Vacuolar storage proteins are sorted in the *cis*-cisternae of the pea cotyledon Golgi apparatus. J. Cell Biol. **152,** 41–50.

Holwerda, B., Padgett, H., and Rogers, J. (1992). Proaleurain vacuolar targeting is mediated by short contiguous peptide interactions. Plant Cell **4,** 307–318.

Horsley, D., Coleman, J., Evans, D., Crooks, K., Peart, J., Satiat-Jeunemaitre, B., and Hawes, C. (1993). A monoclonal antibody, JIM84, recognizes the Golgi apparatus and plasma membrane in plant cells. J. Exp. Bot. **44,** 223–229.

Kahn, R., and Gilman, A. (1986). The protein cofactor necessary for ADP-ribosylation of Gs by cholera toxin is itself a GTP binding protein. J. Biol. Chem. **261,** 7906–7911.

Kaneko, T., Watanabe, R., Sato, M., Osumi, M., and Takatsuki, A. (1994). Morphological changes in Golgi apparatus induced by brefeldin A treatment in tobacco protoplasts. Plant Morphol. **6,** 1–11.

Kim, D.H., Eu, Y.J., Yoo, C.M., Kim, Y.W., Pih, K.T., Jin, J.B., Kim, S.J., Stenmark, H., and Hwang, I.I. (2001). Trafficking of phosphatidylinositol 3-phosphate from the *trans*-Golgi network to the lumen of the central vacuole in plant cells. Plant Cell **13,** 287–301.

Kimura, S., Yamada, M., Igaue, I., and Mitsui, T. (1993). Structure and function of the Golgi complex in rice cells: Characterization of Golgi membrane glycoproteins. Plant Cell Physiol. **34,** 855–863.

Klausner, R., Donaldson, J., and Lippincott-Schwartz, J. (1992). Brefeldin A: Insights into the control of membrane traffic and organelle structure. J. Cell Biol. **116,** 1071–1080.

Kunze, I., Hillmer, S., Kunze, G., and Muentz, K. (1995). Brefeldin A differentially affects protein secretion from suspension-cultured tobacco cells (*Nicotiana tabacum*). J. Plant Physiol. **146,** 71–80.

Linsmaier, E.M., and Skoog, F. (1965). Organic growth factor requirements of tobacco tissue culture. Physiol. Plant. **18,** 100–127.

Lippincott-Schwartz, J., Yuan, L., Bonifacino, J., and Klausner, R. (1989). Rapid redistribution of Golgi proteins into the ER in cells treated with brefeldin A: Evidence for membrane cycling from Golgi to ER. Cell **56,** 801–813.

Lippincott-Schwartz, J., Roberts, T.H., and Hirschberg, K. (2000). Secretory protein trafficking and organelle dynamics in living cells. Annu. Rev. Cell Dev. Biol. **16,** 557–589.

Mansour, S., Skaug, J., Zhao, X., Giordano, J., Scherer, S., and Melancon, P. (1999). p200 ARF-GEP1: A Golgi-localized guanine nucleotide exchange protein whose Sec7 domain is targeted by the drug brefeldin A. Proc. Natl. Acad. Sci. USA **96,** 7968–7973.

Martinez-Menarguez, J.A., Geuze, H.J., Slot, J.W., and Klumpermann. J.A. (1999). Vesicular tubular clusters between the ER and Golgi mediate concentration of soluble secretory proteins by exclusion from COP-I coated vesicles. Cell **98,** 81–90.

Marty, F. (1999). Plant vacuoles. Plant Cell **11,** 587–600.

Melancon, P., Clarke, A., and Yan, Y.P. (1997). GBF1: A Golgi-specific Sec7p-related brefeldin A resistance factor. Mol. Biol. Cell Suppl. **8,** 1383a.

Moss, J., and Vaughn, M. (1998). Molecules in the ARF orbit. J. Biol. Chem. **273,** 21431–21434.

Movafeghi, A., Happel, N., Pimpl, P., Tai, G.-H., and Robinson, D.G. (1999). *Arabidopsis* Sec21p and Sec23p homologs: Probable coat proteins of plant COP-coated vesicles. Plant Physiol. **119,** 1437–1445.

Mullen, R., Lisenbee, C., Miernyk, J., and Trelease, R. (1999). Peroxisomal membrane ascorbate peroxidase is sorted to a membranous network that resembles a subdomain of the endoplasmic reticulum. Plant Cell **11,** 2167–2185.

Murashige, T., and Skoog, F. (1962). A revised medium for growth and rapid bioassays with tobacco tissue culture. Physiol. Plant. **15,** 473–497.

Narula, N., McMorrow, I., Plopper, G., Doherty, J., Matlin, K., Burke, B., and Stow, J. (1992). Identification of a 200-kD, brefeldin-sensitive protein on Golgi membranes. J. Cell Biol. **117,** 27–38.

Nebenführ, A., and Staehelin, L.A. (2001). Mobile factories: Golgi dynamics in plant cells. Trends Plant Sci. **6,** 160–167.

Nebenführ, A., Gallagher, L., Dunahay, T.G., Frohlick, J.A., Masurkiewicz, A.M., Meehl, J.B., and Staehelin, L.A. (1999). Stop-and-go movements of plant Golgi stacks are mediated by the acto-myosin system. Plant Physiol. **121,** 1127–1141.

Nebenführ, A., Frohlick, J.A., and Staehelin, L.A. (2000). Redistribution of Golgi stacks and other organelles during mitosis and cytokinesis in plant cells. Plant Physiol. **124,** 135–151.

Nickel, W., and Brügger, B. (1999). COPI-mediated protein and lipid sorting in the early secretory pathway. Protoplasma **207,** 115–124.

Noguchi, T., and Watanabe, H. (1999). Brefeldin A effects on the *trans*-Golgi network and Golgi bodies in *Botryococcus* are not uniform during the cell cycle. Protoplasma **209,** 193–206.

Oprins, A., Duden, R., Kreis, T.E., Geuze, H.J., and Slot, J.W. (1993). β-COP localizes mainly to the *cis*-Golgi side in exocrine pancreas. J. Cell Biol. **121,** 49–59.

Orci, L., Amherdt, M., Ravazzola, M., Perrelet, A., and Rothman, J. (2000a). Exclusion of Golgi residents from transport vesicles budding from Golgi cisternae in intact cells. J. Cell Biol. **150,** 1263–1270.

Orci, L., Ravazzola, M., Volchuk, A., Engel, T., Gmachl, M., Amherdt, M., Perrelet, A., Söllner, T.H., and Rothman, J.E. (2000b). Anterograde flow of cargo across the Golgi stack potentially mediated via bidirectional "percolating" COPI vesicles. Proc. Natl. Acad. Sci. USA **97,** 10400–10405.

Pagny, S., Cabanes-Macheteau, M., Gillikin, J.W., Leborgne-Castel, N., Lerouge, P., Boston, R.S., Faye, L., and Gomord, V. (2000). Protein recycling from the Golgi apparatus to the endoplasmic reticulum in plants and its minor contribution to calreticulin retention. Plant Cell **12,** 739–755.

Pelham, H.R.B., and Rothman, J.E. (2000). The debate about transport in the Golgi: Two sides of the same coin? Cell **102,** 713–719.

Peters, P.J., Hsu, V.W., Ooi, C.E., Finazzi, D., Teal, S.B., Oorschot, V., Donaldson, J.G., and Klausner, R.D. (1995). Overexpression of wild type and mutant ARF1 and ARF6: Distinct perturbations of non-overlapping membrane compartments. J. Cell Biol. **122,** 1155–1167.

Pimpl, P., Movafeghi, A., Coughlan, S., Denecke, J., Hillmer, S., and Robinson, D.G. (2000). In situ localization and in vitro induction of plant COPI-coated vesicles. Plant Cell **12,** 2219–2236.

Randazzo, P.A., Yang, Y.C., Rulka, C., and Kahn, R.A. (1993). Activation of ADP-ribosylation factor by Golgi membranes: Evidence for a brefeldin A– and protease-sensitive activating factor on Golgi membranes. J. Biol. Chem. **268,** 9555–9563.

Robineau, S., Chabre, M., and Antonny, B. (2000). Binding site of brefeldin A at the interface between the small G protein ADP-ribosylation factor 1 (ARF1) and the nucleotide-exchange factor Sec7 domain. Proc. Natl. Acad. Sci. USA **97,** 9913–9918.

Robinson, D., Bäumer, M., Hinz, G., and Hohl, I. (1997). Ultrastructure of the pea cotyledon Golgi apparatus: Origin of dense vesicles and the action of brefeldin A. Protoplasma **200,** 198–209.

Robinson, D.G., Hinz, G., and Holstein, S.E.H. (1998). The molecular characterization of transport vesicles. Plant Mol. Biol. **38,** 47–76.

Robinson, M.S., and Kreis, T.E. (1992). Recruitment of coat proteins onto Golgi membranes in intact and permeabilized cells: Effects of brefeldin A and G protein activators. Cell **69,** 129–138.

Rutten, T., and Knuiman, B. (1993). Brefeldin A effects on tobacco pollen tubes. Eur. J. Cell Biol. **61,** 247–255.

Salomon, S., and Meindl, U. (1996). Brefeldin A induces reversible dissociation of the Golgi apparatus in the alga *Micrasterias*. Protoplasma **194,** 231–242.

Samuels, A.L., Giddings, T.H., and Staehelin, L.A. (1995). Cytokinesis in tobacco BY-2 and root tip cells: A new model of cell plate formation in higher plants. J. Cell Biol. **130,** 1345–1357.

Sanderfoot, A.A., Assaad, F.F., and Raikhel, N.V. (2000). The *Arabidopsis* genome: An abundance of soluble *N*-ethylmaleimide–sensitive factor adaptor protein receptors. Plant Physiol. **124,** 1558–1569.

Satiat-Jeunemaitre, B., and Hawes, C. (1992). Redistribution of a Golgi glycoprotein in plant cells treated with brefeldin A. J. Cell Sci. **103,** 1153–1166.

Satiat-Jeunemaitre, B., Cole, L., Bouret, T., Howard, R., and Hawes, C. (1996). Brefeldin A effects in plant and fungal cells: Something new about vesicle trafficking? J. Microsc. **181,** 162–177.

Scales, S.J., Gomez, M., and Kreis, T.E. (2000). Coat proteins regulating membrane traffic. Int. Rev. Cytol. **195,** 67–144.

Scheel, J., Pepperkok, R., Lowe, M., Griffiths, G., and Kreis, T. (1997). Dissociation of coatomer from membranes is required for brefeldin A–induced transfer of Golgi enzymes to the endoplasmic reticulum. J. Cell Biol. **137,** 319–333.

Schindler, T., Bergfeld, R., Hohl, M., and Schopfer, P. (1994). Inhibition of Golgi apparatus function by brefeldin A in maize coleoptiles and its consequences on auxin mediated growth, cell wall extensibility, and secretion of cell wall proteins. Planta **192,** 404–413.

Sciaky, N., Presley, J., Smith, C., Zaal, K.J.M., Cole, N., Moreira, J.E., Terasaki, M., Siggia, E., and Lippincott-Schwartz, J. (1997). Golgi tubule traffic and the effects of brefeldin A visualized in living cells. J. Cell Biol. **139,** 1137–1155.

Seemann, J., Jokitalo, E., Pypaert, M., and Warren, G. (2000). Matrix proteins can generate the higher order architecture of the Golgi apparatus. Nature **407,** 1022–1026.

Serafini, T., Orci, L., Amherdt, M., Brunner, M., Kahn, R., and Rothman, J. (1991). ADP-ribosylation factor is a subunit of the coat of Golgi-derived COP-coated vesicles: A novel role for a GTP-binding protein. Cell **67,** 239–253.

Staehelin, A., and Driouich, A. (1997). Brefeldin A effects in plants: Are different Golgi responses caused by different sites of action? Plant Physiol. **114,** 401–403.

Staehelin, L.A., Giddings, T.H., Kiss, J.Z., and Sack, F.D. (1990). Macromolecular differentiation of Golgi stacks in root tips of *Arabidopsis* and *Nicotiana* seedlings as visualized in high pressure frozen and freeze-substituted samples. Protoplasma **157,** 75–91.

Stearns, T., Willingham, M.C., Botstein, D., and Kahn, R.A. (1990). ADP-ribosylation factor is functionally and physically associated with the Golgi complex. Proc. Natl. Acad. Sci. USA **87,** 1238–1242.

Togawa, A., Morinaga, N., Ogasawara, M., Moss, J., and Vaughan, M. (1999). Purification and cloning of a brefeldin A-inhibited guanine nucleotide-exchange protein for ADP-ribosylation factors. J. Biol. Chem. **274,** 12308–12315.

Toomre, D., Keller, P., White, J., Olivo, J.-C., and Simons, K. (1999). Dual-color visualization of *trans*-Golgi network to plasma membrane traffic along microtubules in living cells. J. Cell Sci. **112,** 21–33.

Traub, L.M., Ostrom, J.A., and Kornfeld, S. (1993). Biochemical dissection of AP-1 recruitment onto Golgi membranes. J. Cell Biol. **123,** 561–573.

van Meer, G. (1998). Lipids of the Golgi membrane. Trends Cell Biol. **8,** 29–33.

Vitale, A., and Denecke, J. (1999). The endoplasmic reticulum: Gateway of the secretory pathway. Plant Cell **11,** 615–628.

Vitale, A., and Raikhel, N.V. (1999). What do proteins need to reach different vacuoles? Trends Plant Sci. **4,** 149–155.

Volchuk, A., Amherdt, M., Ravazzola, M., Brugger, B., Rivera, V., Clackson, T., Perrelet, A., Sollner, T., Rothman, J., and Orci, L. (2000). Megavesicles implicated in the rapid transport of intracisternal aggregates across the Golgi stack. Cell **102,** 335–348.

Waters, M.G., Serafini, T., and Rothman, J.E. (1991). A cytosolic protein complex containing subunits of non-clathrin-coated Golgi-transport vesicles. Nature **349,** 248–251.

Wessel, D., and Flügge, U.I. (1984). A method for the quantitative recovery of proteins in dilute solutions in the presence of detergents and lipids. Ann. Biochem. **138,** 141–143.

Yasuhara, H., Sonobe, S., and Shibaoka, H. (1995). Effects of brefeldin A on the formation of the cell plate in tobacco BY-2 cells. Eur. J. Cell Biol. **66,** 274–281.

Zaal, K.J.M., Smith, C.L., Polishchuck, R.S., Altan, N., Cole, N.B., Ellenberg, J., Hirschberg, K., Presley, J.F., Roberts, T.H., Siggia, E., Phair, R.D., and Lippincott-Schwartz, J. (1999). Golgi membranes are absorbed into and reemerge from the ER during mitosis. Cell **99,** 589–601.

Zhang, G.F., and Staehelin, L.A. (1992). Functional compartmentation of the Golgi apparatus of plant cells: Immunocytochemical analysis of high-pressure frozen and freeze-substituted sycamore maple suspension culture cells. Plant Physiol. **99,** 1070–1083.